

Calibration Attention: Learning Reliability-Aware Representations for Vision Transformers

Wenhao Liang¹, Lin Yue¹, Wei Emma Zhang¹, Miao Xu²
Mingyu Guo¹, Olaf Maennel¹, Weitong Chen¹

¹Adelaide University

²The University of Queensland

Abstract

Most calibration methods operate at the logit level, implicitly assuming that miscalibration can be corrected without changing the underlying representation. We challenge this assumption and propose **Calibration Attention (CalAttn)**, a *representation-aware* calibration module for vision transformers that couples instance-wise temperature scaling to transformer token geometry under a proper scoring objective. CalAttn predicts a sample-specific temperature from the [CLS] token and backpropagates calibration gradients into the backbone, thereby reshaping the uncertainty structure of the representation rather than post-hoc adjusting confidence. This yields *token-conditioned uncertainty modulation* with negligible overhead ($< 0.1\%$ additional parameters). Across multiple datasets with ViT/DeiT/Swin backbones, CalAttn consistently improves calibration while preserving accuracy, achieving relative ECE reductions of 3.7% to 77.7% over strong baselines across diverse training objectives. Our results indicate that treating calibration as a representation-level problem is a practical and effective direction for trustworthy uncertainty estimation in transformers.

1 Introduction

A probabilistic classifier is *well calibrated* when its predicted confidence matches empirical correctness: among predictions assigned confidence p , roughly a p fraction are correct. Calibration is therefore central to decision-making under risk and is consequential in safety-critical settings such as medical diagnosis, autonomous driving, and finance [Mehrtash *et al.*, 2020; Feng *et al.*, 2021; Liang *et al.*, 2024b].

Limitations of logit-level calibration. Despite strong accuracy, modern deep networks—including Vision Transformers (ViTs)—are often miscalibrated [Guo *et al.*, 2017; Minderer *et al.*, 2021; Ovadia *et al.*, 2019]. The canonical remedy, temperature scaling (TS), fits a single scalar temperature on a validation set and rescales logits at test time. While simple and effective in-distribution, TS implicitly assumes that miscalibration is (i) *homogeneous* across in-

puts and (ii) *expressible* as a logit-only correction. In practice, predictive uncertainty is heterogeneous and distribution-dependent: different samples exhibit different ambiguity, and shifts in data distribution can substantially change uncertainty patterns [Ovadia *et al.*, 2019]. Consequently, a global temperature can over-dampen genuinely confident predictions while under-correcting ambiguous ones, producing brittle calibration under distribution shift even when accuracy remains high. Training-time approaches (e.g., label smoothing, focal-style objectives, and differentiable calibration surrogates) mitigate miscalibration but typically rely on static hyperparameters and do not explicitly condition uncertainty on the learned representation [Mukhoti *et al.*, 2020a; Müller *et al.*, 2019; Tao *et al.*, 2023; Liang *et al.*, 2024a].

Representation geometry as a source of uncertainty. We argue that, in transformers, miscalibration is not solely an artifact of the output layer but is tied to the geometry of the learned representation. ViTs aggregate global evidence into the [CLS] token, which summarizes patch information and encodes signals related to class separability, sample ambiguity, and distributional irregularities. These signals are largely invisible to post-hoc logit transformations. This motivates the view that *calibration should be conditioned on internal token geometry*, rather than treated purely as a logit correction.

Representation-aware calibration. Motivated by this perspective, we introduce *representation-aware calibration*: an end-to-end paradigm in which uncertainty modulation is modeled as a function of internal token representations. Concretely, we propose **Calibration Attention (CalAttn)**, a lightweight two-layer MLP that predicts an instance-specific temperature from the [CLS] embedding and rescales logits accordingly:

$$T(x) = g_\phi(\text{CLS}_\theta(x)),$$

where g_ϕ is trained jointly with backbone parameters θ . This design couples calibration with representation learning: calibration gradients propagate through the [CLS] channel, enabling the backbone to adjust its uncertainty geometry during training. In contrast to adaptive temperature scaling variants that regress temperatures from logits or apply post-hoc corrections on frozen features, CalAttn explicitly links token learning dynamics with uncertainty estimation in ViTs.

Contributions. Our contributions are:

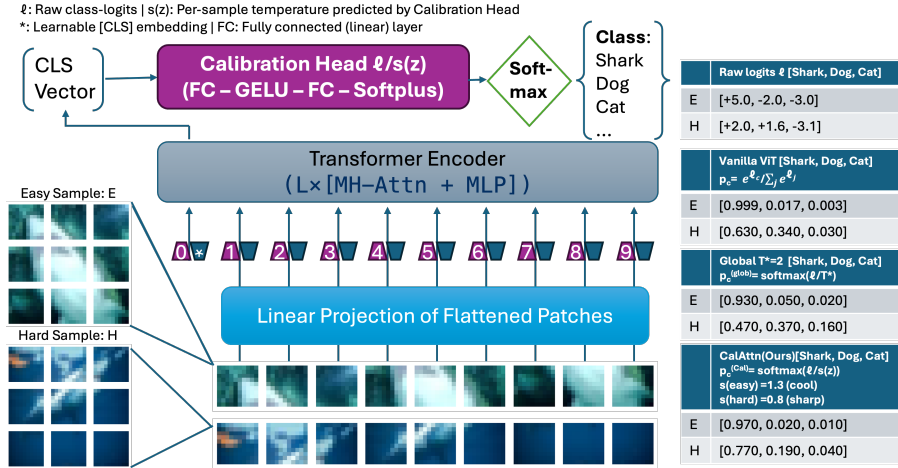


Figure 1: **Vision Transformer with Calibration Attention.** A lightweight calibration head reads the final [CLS] token and predicts a strictly positive, per-sample temperature $s(\mathbf{z})$. The class logits produced by the standard classifier head are divided by this scale prior to the softmax, enabling representation-conditioned cooling or sharpening of predictive confidence. CalAttn learns reliability-aware representations by conditioning confidence on the [CLS] embedding, replacing global post-hoc temperature scaling.

- **Paradigm.** We formalize **representation-aware calibration** for transformers, where uncertainty modulation is conditioned on internal token geometry rather than applied as a purely logit-level post-hoc transform.
- **Method.** We propose **Calibration Attention (CalAttn)**, a minimal module that predicts sample-specific temperatures from [CLS] and injects calibration gradients into representation via a proper scoring objective.
- **Evidence.** Across MNIST, CIFAR-10/100, Tiny-ImageNet, and ImageNet-1K, and across ViT/DeiT/Swin backbones, CalAttn consistently improves calibration while preserving accuracy and remains complementary to standard post-hoc methods.

2 Method

We aim to replace post-hoc *global* temperature scaling with an *instance-wise, representation-conditioned* temperature that is learned jointly with the backbone. Given an input image, a ViT produces a final-layer [CLS] embedding that summarizes global evidence. CalAttn attaches a lightweight temperature head to this embedding, predicts a strictly positive scale for each sample, rescales logits before the softmax, and trains end-to-end with a calibration-aware proper scoring objective. This coupling ensures that calibration gradients propagate through the [CLS] pathway and can reshape the representation during training, rather than only correcting confidence after the fact. Figure 1 provides an overview; notation is summarized in Appendix A.

2.1 Preliminaries

ViT predictions. Given an input image $\mathbf{x} \in \mathbb{R}^{3 \times H \times W}$, a Vision Transformer prepends a learned [CLS] token and, after L encoder blocks, outputs the final [CLS] embedding $\mathbf{z}_{\text{CLS}} \in \mathbb{R}^d$. A linear classifier head produces logits

$$\ell = \mathbf{W}_{\text{cls}} \mathbf{z}_{\text{CLS}} + b_{\text{cls}} \in \mathbb{R}^C,$$

which define probabilities via the temperature-scaled softmax

$$\sigma_i(\ell, T) = \frac{\exp(\ell_i/T)}{\sum_{j=1}^C \exp(\ell_j/T)}.$$

Global temperature scaling. Temperature scaling (TS) fits a single scalar T^* on a validation set and applies it at test time [Guo *et al.*, 2017]. This procedure is decoupled from representation learning and cannot condition confidence adjustment on sample-specific uncertainty. Under heterogeneous uncertainty or distribution shift, a single global temperature may under-correct ambiguous samples while over-smoothing confident ones.

2.2 Calibration Attention

Instance-wise, representation-conditioned temperature. Let $\mathbf{z} \triangleq \mathbf{z}_{\text{CLS}}$ denote the final [CLS] embedding. CalAttn predicts each *scale* (temperature) via a two-layer MLP:

$$s(\mathbf{z}) = \text{Softplus}(\mathbf{w}_2^\top \text{GELU}(\mathbf{W}_1 \mathbf{z}) + b_2) + \varepsilon, \quad (1)$$

where $\mathbf{W}_1 \in \mathbb{R}^{h \times d}$, $\mathbf{w}_2 \in \mathbb{R}^h$, $b_2 \in \mathbb{R}$, and $\varepsilon = 10^{-6}$ ensures strict positivity. We use an identity-preserving initialization with $\mathbf{w}_2 = 0$ and $b_2 = \ln(e^1 - 1)$ such that $s(\mathbf{z}) \approx 1$ at the start of training, making CalAttn initially equivalent to the baseline model. The calibrated predictive distribution is

$$\hat{\mathbf{y}} = \text{softmax}(\ell/s(\mathbf{z})). \quad (2)$$

Since scaling preserves logit ordering, CalAttn primarily modulates confidence rather than class ranking.

Calibration-aware proper scoring objective. We train the backbone and CalAttn jointly by minimizing a proper scoring objective consisting of cross-entropy and a Brier term:

$$\mathcal{L} = \mathcal{L}_{\text{CE}}(\hat{\mathbf{y}}, y) + \lambda \|\hat{\mathbf{y}} - \mathbf{e}_y\|_2^2, \quad (3)$$

where \mathbf{e}_y is the one-hot label and $\lambda = 0.1$ unless stated otherwise. The Brier term acts as a differentiable surrogate encouraging calibrated probabilities, and its gradients back-propagate through $s(\mathbf{z})$ into the [CLS] representation (see Appendix E).

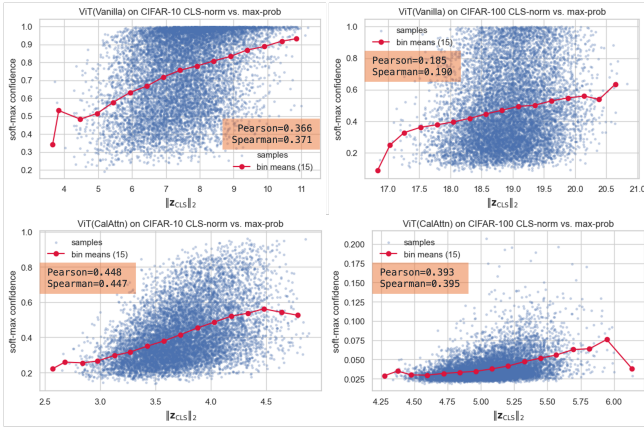


Figure 2: $[\text{CLS}]$ ℓ_2 -norm versus maximum softmax probability on CIFAR-10/100. Blue dots are samples; red curves show bin means. Correlation is moderate and non-deterministic, motivating learning a representation-aware calibration function.

Algorithm 1 Per-sample Temperature Scaling with CalAttn

Input: $[\text{CLS}]$ token $\mathbf{z}_{\text{cls}} \in \mathbb{R}^d$, logits $\ell \in \mathbb{R}^C$

Parameters: $W_1 \in \mathbb{R}^{h \times d}$, $W_2 \in \mathbb{R}^{1 \times h}$, $b_2 = \ln(e^1 - 1)$, $\varepsilon = 10^{-6}$

Output:

Calibrated probabilities $\hat{\mathbf{y}} \in \mathbb{R}^C$

- 1: $\mathbf{h} \leftarrow \text{GELU}(W_1 \mathbf{z}_{\text{cls}})$ {first FC: $d \rightarrow h$ }
 - 2: $s \leftarrow \text{Softplus}(W_2 \mathbf{h} + b_2) + \varepsilon$ $\{s > 0\}$
 - 3: $\ell^{\text{cal}} \leftarrow \ell / s$ {cool/sharpen logits}
 - 4: $\hat{\mathbf{y}} \leftarrow \text{softmax}(\ell^{\text{cal}})$
 - 5: **return** $\hat{\mathbf{y}}$
-

Gradient signal through the temperature head. Differentiating \mathcal{L} with respect to the (positive) scale s yields

$$\frac{\partial \mathcal{L}}{\partial s} = \underbrace{\frac{\ell_y - \sum_j \hat{y}_j \ell_j}{s^2}}_{\text{CE term}} + \underbrace{\lambda \frac{\partial}{\partial s} \|\hat{\mathbf{y}} - \mathbf{e}_y\|_2^2}_{\text{Brier term}}. \quad (4)$$

Using the softmax Jacobian $J(\hat{\mathbf{y}}) = \text{diag}(\hat{\mathbf{y}}) - \hat{\mathbf{y}}\hat{\mathbf{y}}^\top$, the Brier contribution can be written as

$$\frac{\partial}{\partial s} \|\hat{\mathbf{y}} - \mathbf{e}_y\|_2^2 = -\frac{2}{s^2} (\hat{\mathbf{y}} - \mathbf{e}_y)^\top J(\hat{\mathbf{y}}) \ell. \quad (5)$$

2.3 $[\text{CLS}]$ Token as an Uncertainty Carrier

The $[\text{CLS}]$ token aggregates global context across patches and layers. Prior work suggests that its geometry encodes signals related to separability, sample difficulty, and robustness [Naseer *et al.*, 2021; Zhou *et al.*, 2022; Minderer *et al.*, 2021]. CalAttn leverages the full embedding to learn a non-linear mapping from representation to uncertainty modulation, rather than relying on a single handcrafted statistic. At inference, CalAttn adds a single lightweight head: compute $s(\mathbf{z})$, rescale logits, and apply softmax (Algorithm 1).

3 Experiments

This section provides a comprehensive evaluation of CalAttn across architectures, datasets, and calibration criteria

¹. We first report in-distribution calibration and accuracy on CIFAR-10/100, MNIST, and Tiny-ImageNet using ViT, DeiT, and Swin backbones, including results both before and after post-hoc temperature scaling. We then analyze reliability diagrams and high-confidence errors to assess safety-critical behavior. Next, we study robustness under distribution shift. We further evaluate scalability on ImageNet-1K and conduct extensive ablations on calibration head design, λ trade-off parameter, and choice of representation used to predict temperatures. Finally, we compare CalAttn with post-hoc instance-wise methods to quantify the benefits of learning calibration.

3.1 Experimental Set-up

Datasets. We consider CIFAR-10/100 (50k/10k, 32×32), MNIST, Tiny-ImageNet, and ImageNet-1K, spanning increasing class counts and ambiguity regimes.

Architectures. We evaluate transformer backbones ViT₂₂₄ [Dosovitskiy *et al.*, 2021], DeiT-S [Touvron *et al.*, 2021], and Swin-S [Liu *et al.*, 2021]. Unless explicitly stated, CalAttn augments each transformer with a single temperature head while keeping the backbone and classifier head unchanged. (We additionally include CNN baselines where relevant for comparison to prior instance-wise calibration baselines.)

Training protocol. Unless stated otherwise, models are trained for 350 epochs with SGD (momentum 0.9, weight decay 5×10^{-4}) and a step learning-rate schedule: 0.1 for first 150 epochs, 0.01 for next 100 epochs, and 0.001 for final 100 epochs. We use standard augmentation and optimization settings recommended for each backbone. CalAttn uses $\lambda = 0.1$ in Eq. (3) throughout and we do not tune λ per dataset.

Baselines. We re-implement representative train-time objectives including weight decay (WD) [Guo *et al.*, 2017], Brier score (BS) [Brier, 1950], MMCE [Kumar *et al.*, 2018], label smoothing (LS) [Szegedy *et al.*, 2016], FocalLoss-53 [Mukhoti *et al.*, 2020a], and Dual Focal Loss (DFL) [Tao *et al.*, 2023]. We also report CE+ λ BS (without CalAttn) to isolate the effect of using a strictly proper auxiliary term from the effect of representation-conditioned scaling. For sample-dependent scaling baselines, we include SATS [Joy *et al.*, 2023] and Relaxed Softmax [Neumann *et al.*, 2018].

Post-hoc temperature scaling (TS). For each trained model, TS fits a single scalar temperature T^* on a held-out validation split (5% of the training data). Following [Mukhoti *et al.*, 2020a], we select $T^* \in \{0.1, 0.2, \dots, 10.0\}$ by grid search to minimize validation ECE (15 equal-width bins).

3.2 Main Results on ECE: before and after TS

Table 1 reports ECE before and after applying temperature scaling (TS) and CalAttn yields consistent reductions (mostly negative $\Delta\%$ in Fig. 3). We highlight three findings.

¹Code for the experiments is available at <https://anonymous.4open.science/r/CalibrationAttention-CalAttn--D2B8>.

²Temperature scaling fits a single scalar T^* on a held-out validation split (5% of training data) by grid search over $T \in \{0.1, 0.2, \dots, 10.0\}$ to minimize validation ECE (15 equal-width bins), following [Mukhoti *et al.*, 2020a] and utilizing their public code [Mukhoti *et al.*, 2020b]. Parentheses in Post-T report T^* .

Table 1: \downarrow ECE (%) before and after applying global temperature scaling (15 bins)².

| Dataset | Model | Weight Decay [Guo <i>et al.</i> , 2017] | | Brier Loss [Brier, 1950] | | MMCE [Kumar <i>et al.</i> , 2018] | | Label Smooth [Szegedy <i>et al.</i> , 2016] | | Focal Loss - 53 [Mukhoti <i>et al.</i> , 2020a] | | Dual Focal [Tao <i>et al.</i> , 2023] | | CE + λ BS ($\lambda = 0.1$) | |
|--------------------------------------|--------------------------------------|--------------------------------------------|-------------------|-----------------------------|-------------------|--------------------------------------|-------------------|------------------------------------------------|-------------------|----------------------------------------------------|-------------------|------------------------------------------|-------------------|------------------------------------------|-------------------|
| | | Pre T | Post-T (T*) | Pre T | Post-T (T*) | Pre T | Post-T (T*) | Pre T | Post-T (T*) | Pre T | Post-T (T*) | Pre T | Post-T (T*) | Pre T | Post-T (T*) |
| CIFAR-100 | ResNet-50 | 18.02 | 2.60(2.20) | 5.47 | 3.71(1.10) | 15.05 | 3.41(1.90) | 6.38 | 5.12(1.10) | 5.54 | 2.28(1.10) | 8.79 | 2.31(1.30) | 14.41 | 2.35(1.60) |
| | ResNet-110 | 19.29 | 4.75(2.30) | 6.72 | 3.59(1.20) | 18.84 | 4.52(2.30) | 9.53 | 5.20(1.30) | 11.02 | 3.88(1.30) | 11.65 | 3.75(1.30) | 19.36 | 3.38(1.80) |
| | Wide-ResNet-26-10 | 15.17 | 2.82(2.10) | 4.07 | 3.03(1.10) | 13.57 | 3.89(2.00) | 3.29 | 3.29(1.00) | 2.62 | 2.16(1.10) | 5.30 | 2.27(1.20) | 6.63 | 5.24(1.20) |
| | DenseNet-121 | 19.07 | 3.42(2.20) | 4.28 | 2.22(1.10) | 17.37 | 3.22(2.00) | 8.63 | 4.82(1.10) | 3.40 | 1.55(1.10) | 6.69 | 1.65(1.20) | 16.10 | 2.95(1.60) |
| | ViT ₂₂₄ | 13.11 | 3.30(1.30) | 2.99 | 2.99(1.00) | 11.52 | 2.34(1.30) | 8.33 | 2.24(1.10) | 5.33 | 3.46(1.10) | 3.42 | 3.42(1.00) | 6.89 | 3.49(1.50) |
| | ViT ₂₂₄ +CalAttn(Ours) | 8.25 | 1.85(1.20) | 1.98 | 2.15(1.10) | 9.04 | 2.22(1.20) | 2.09 | 2.09(1.00) | 2.61 | 2.61(1.00) | 3.72 | 1.92(1.10) | 4.09 | 1.49(1.10) |
| | DeiT _{small} | 7.46 | 3.54(1.10) | 2.17 | 2.17(1.00) | 7.88 | 2.55(1.20) | 1.75 | 1.75(1.00) | 3.27 | 3.27(1.00) | 3.30 | 2.19(1.10) | 5.46 | 3.86(1.40) |
| | DeiT _{small} +CalAttn(Ours) | 6.87 | 1.48(1.20) | 1.98 | 2.19(1.10) | 6.51 | 1.86(1.20) | 1.55 | 1.55(1.00) | 3.15 | 3.15(1.00) | 1.93 | 1.93(1.00) | 2.88 | 0.86(1.10) |
| | Swin _{small} | 3.51 | 2.46(0.90) | 2.54 | 2.54(1.00) | 3.53 | 2.78(0.90) | 9.00 | 2.41(0.80) | 10.64 | 2.51(0.80) | 8.18 | 3.15(0.80) | 4.59 | 2.51(1.20) |
| | Swin _{small} +CalAttn(Ours) | 1.93 | 1.93(1.00) | 3.03 | 2.02(1.10) | 1.92 | 1.92(1.00) | 6.59 | 2.57(0.90) | 6.15 | 3.17(0.90) | 3.97 | 3.21(0.90) | 1.51 | 1.51(1.00) |
| CIFAR-10 | ResNet-50 | 4.23 | 1.37(2.50) | 1.83 | 0.96(1.10) | 4.67 | 1.11(2.60) | 4.23 | 1.87(0.90) | 1.46 | 1.46(1.00) | 1.32 | 1.32(1.00) | 5.71 | 1.53(1.90) |
| | ResNet-110 | 4.86 | 1.94(2.60) | 2.50 | 1.36(1.20) | 5.22 | 1.24(2.80) | 3.74 | 1.22(0.90) | 1.67 | 1.10(1.10) | 1.48 | 1.27(1.10) | 6.23 | 2.29(1.90) |
| | Wide-ResNet-26-10 | 3.24 | 1.86(2.20) | 1.17 | 1.17(1.00) | 3.60 | 1.26(2.20) | 4.66 | 1.27(0.80) | 1.83 | 1.17(0.90) | 3.35 | 0.94(0.80) | 3.49 | 1.15(1.50) |
| | DenseNet-121 | 4.70 | 1.54(2.40) | 1.24 | 1.24(1.00) | 4.97 | 1.71(2.40) | 4.05 | 1.01(0.90) | 1.73 | 1.22(0.90) | 0.70 | 1.31(0.90) | 5.16 | 1.83(1.60) |
| | ViT ₂₂₄ | 7.39 | 1.68(1.30) | 1.87 | 1.87(1.00) | 3.47 | 1.06(1.10) | 1.79 | 1.79(1.00) | 8.70 | 2.11(0.70) | 3.71 | 2.15(0.90) | 3.98 | 3.41(1.40) |
| | ViT ₂₂₄ +CalAttn(Ours) | 4.76 | 1.38(1.20) | 2.62 | 1.77(1.10) | 4.36 | 1.64(1.20) | 2.58 | 1.55(0.90) | 10.04 | 2.06(0.70) | 4.57 | 2.86(0.90) | 1.56 | 1.21(1.10) |
| | DeiT _{small} | 4.42 | 1.52(1.20) | 2.02 | 2.02(1.00) | 6.01 | 1.78(1.20) | 1.84 | 1.84(1.00) | 10.65 | 2.79(0.70) | 5.11 | 2.79(0.80) | 4.25 | 2.95(1.30) |
| | DeiT _{small} +CalAttn(Ours) | 4.10 | 1.67(1.10) | 1.98 | 1.32(1.10) | 3.57 | 1.32(1.10) | 2.41 | 2.41(1.00) | 9.91 | 1.94(0.70) | 3.87 | 2.84(0.90) | 1.88 | 1.22(1.10) |
| | Swin _{small} | 1.95 | 1.91(0.90) | 1.12 | 1.12(1.00) | 1.73 | 2.31(0.90) | 6.71 | 1.45(0.80) | 15.70 | 2.32(0.60) | 8.54 | 2.40(0.70) | 2.01 | 1.47(1.20) |
| | Swin _{small} +CalAttn(Ours) | 1.74 | 1.74(1.00) | 1.08 | 1.08(1.00) | 1.00 | 1.00(1.00) | 6.09 | 1.30(0.80) | 14.97 | 1.66(0.60) | 7.50 | 2.32(0.80) | 0.94 | 0.94(1.00) |
| MNIST | ViT ₂₂₄ | 2.91 | 1.15(0.90) | 48.83 | 5.61(8.70) | 19.98 | 5.18(2.10) | 12.77 | 8.07(1.50) | 24.07 | 2.07(1.40) | 18.12 | 4.85(2.30) | 5.34 | 1.08(0.80) |
| | ViT ₂₂₄ +CalAttn(Ours) | 2.73 | 0.99(0.90) | 3.13 | 0.90(0.90) | 3.89 | 1.09(0.80) | 8.29 | 0.99(0.70) | 7.10 | 1.30(0.40) | 18.37 | 1.56(0.50) | 0.74 | 0.44(0.90) |
| | DeiT _{small} | 2.87 | 1.15(0.90) | 28.37 | 2.73(3.20) | 4.66 | 1.16(0.80) | 8.70 | 1.47(0.70) | 21.72 | 2.43(0.50) | 15.90 | 1.55(0.70) | 4.48 | 1.04(0.80) |
| | DeiT _{small} +CalAttn(Ours) | 1.30 | 1.30(1.00) | 1.15 | 0.46(0.90) | 2.11 | 0.92(0.90) | 6.20 | 1.00(0.80) | 18.28 | 1.54(0.50) | 8.96 | 2.28(0.60) | 0.91 | 0.91(1.00) |
| | Swin _{small} | 3.64 | 3.21(1.20) | 1.32 | 0.67(0.90) | 1.26 | 0.67(0.90) | 8.09 | 0.56(0.60) | 7.09 | 1.28(0.50) | 8.78 | 0.49(0.50) | 1.86 | 1.86(1.00) |
| Swin _{small} +CalAttn(Ours) | 0.66 | 0.56(1.10) | 0.85 | 0.45(0.90) | 1.16 | 0.51(0.70) | 6.89 | 0.46(0.60) | 11.75 | 0.84(0.50) | 5.04 | 0.47(0.60) | 0.85 | 0.42(0.90) | |
| Tiny-ImageNet | ViT ₂₂₄ | 22.11 | 1.93(1.90) | 4.44 | 1.89(1.10) | 19.84 | 1.81(1.80) | 2.25 | 1.51(1.10) | 3.28 | 1.93(1.10) | 2.45 | 2.44(1.10) | 1.75 | 1.66(1.10) |
| | ViT ₂₂₄ +CalAttn(Ours) | 4.41 | 3.03(1.10) | 9.18 | 1.78(1.30) | 4.97 | 3.07(1.20) | 2.22 | 1.48(1.10) | 1.68 | 1.14(1.30) | 13.57 | 1.34(1.40) | 1.01 | 0.78(1.10) |
| | DeiT _{small} | 13.04 | 2.13(1.10) | 2.70 | 1.79(1.10) | 13.66 | 1.26(1.10) | 2.36 | 1.64(1.30) | 10.28 | 2.15(1.50) | 9.37 | 1.79(1.30) | 1.69 | 1.55(1.10) |
| | DeiT _{small} +CalAttn(Ours) | 2.37 | 1.38(1.40) | 1.09 | 0.19(1.20) | 2.83 | 1.24(1.50) | 1.64 | 1.20(1.10) | 2.15 | 1.11(1.30) | 1.79 | 0.87(1.30) | 0.95 | 0.83(1.20) |
| | Swin _{small} | 3.03 | 2.76(0.90) | 0.81 | 0.25(0.90) | 1.94 | 1.94(1.00) | 4.92 | 2.41(0.90) | 4.47 | 2.46(0.90) | 4.90 | 2.57(0.90) | 1.52 | 1.52(1.00) |
| Swin _{small} +CalAttn(Ours) | 2.92 | 1.22(1.10) | 0.67 | 0.64(1.10) | 1.41 | 1.41(1.00) | 2.67 | 2.67(1.00) | 2.32 | 2.32(1.00) | 2.29 | 2.29(1.00) | 0.82 | 0.24(0.90) | |

Table 2: Top-1 classification accuracy (%) \uparrow on CIFAR-10 and CIFAR-100 validation set. Baseline denotes cross-entropy training; “+CalAttn” adds the calibration head.

| Backbone | CIFAR-10 | | CIFAR-100 | |
|-----------------------|----------|-------------|-----------|-------------|
| | Baseline | + CalAttn | Baseline | + CalAttn |
| ViT ₂₂₄ | 66.1 | 72.8 | 59.2 | 63.6 |
| DeiT _{small} | 69.4 | 76.1 | 63.9 | 67.5 |
| Swin _{small} | 74.5 | 75.8 | 66.7 | 68.2 |

(1) **Calibration should be considered jointly together with accuracy.** A perfectly calibrated yet inaccurate model is undesirable. We therefore report Top-1 accuracy in Table 2, and NLL alongside calibration metrics in Table 16. CalAttn improves calibration without degrading accuracy; the accuracy change is typically within a small range.

(2) **Representation-conditioned scaling yields consistent gains on transformers.** With $< 0.1\%$ additional parameters (Table 13), CalAttn reduces ECE for ViT/DeiT/Swin across datasets. The gain often remains after TS, indicating that CalAttn improves the underlying confidence structure rather than merely shifting logits by a global scalar.

(3) **High-confidence error analysis.** Beyond ECE, we evaluate high-confidence false positives at threshold 0.90 (HCFP@0.90) and AUROC (Table 3). CalAttn consistently reduces high-confidence mistakes, demonstrating that it mitigates the most safety-critical failure mode (over-confident errors) rather than only improving calibration metrics.

Sensitivity to λ . We sweep $\lambda \in \{0.1, \dots, 1.0\}$ on CIFAR-100 for CE+ λ BS (Table 14) and CE+ λ BS+CalAttn (Table 15)

Table 3: **Effect of CalAttn on high-confidence errors** on CIFAR-100 after post-hoc temperature scaling. Δ (%) is relative change from CE+BS; negative is improvement for error/confidence, positive is improvement for AUROC.

| Backbone | Metric | CE+BS | +CalAttn | Δ (%) |
|----------|-------------------------|-------|----------|--------------|
| ViT-224 | HCFP@0.90 \downarrow | 21.99 | 17.99 | -18.2 |
| | Mean Conf. \downarrow | 97.47 | 92.60 | -5.0 |
| | AUROC \uparrow | 72.26 | 72.47 | +0.3 |
| DeiT-S | HCFP@0.90 \downarrow | 11.99 | 6.99 | -41.7 |
| | Mean Conf. \downarrow | 96.27 | 93.50 | -2.9 |
| | AUROC \uparrow | 77.55 | 78.40 | +1.1 |
| Swin-S | HCFP@0.90 \downarrow | 23.99 | 6.99 | -70.9 |
| | Mean Conf. \downarrow | 94.15 | 92.64 | -1.6 |
| | AUROC \uparrow | 73.71 | 81.94 | +11.2 |

in Appendix I. While the vanilla loss shows mild variation, CalAttn is comparatively insensitive: $\lambda = 0.1$ lies close to the best-performing region, so we fix it to avoid extra hyperparameter tuning and keep comparisons transparent.

3.3 Fine-grained Calibration

ECE with fixed-width binning can obscure localized miscalibration when confidence is skewed or when bins are unevenly populated. We therefore also report smECE (Table 12, Fig. 6), AdaECE (Table 17, Fig. 7), and classwise-ECE (Table 18) in Appendix F, which address complementary issues such as unequal bin occupancy and class imbalance. CalAttn maintains consistent improvements, providing evidence that gains are not an artifact of a specific binning choice.

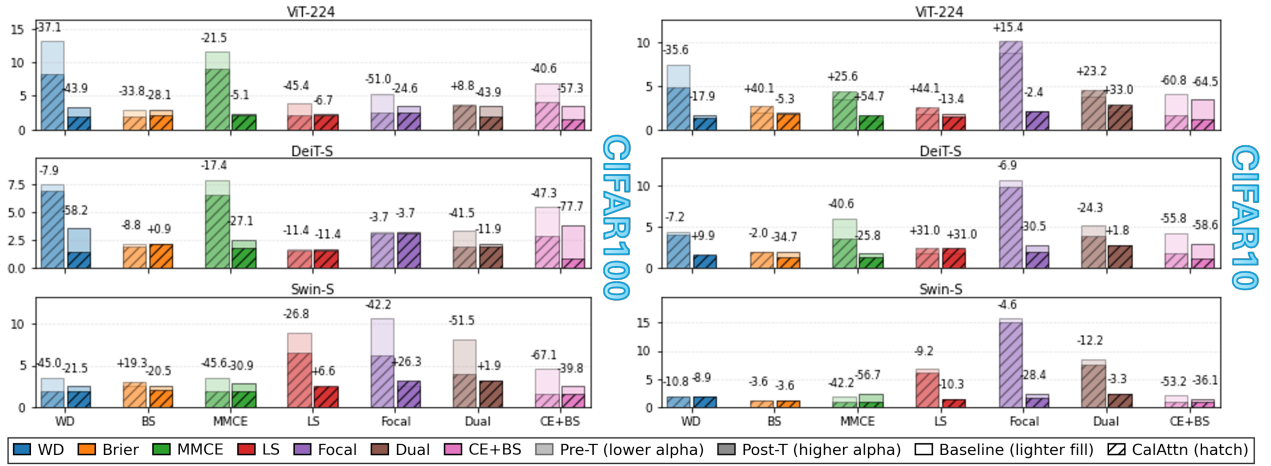


Figure 3: ECE(%) on CIFAR-10/100 across ViT-224, DeiT-S, and Swin-S with relative changes (Δ %, “+” increase, “-” decrease).

3.4 Temporal behavior of CalAttn

Figure 4 tracks the predicted scale $s(x) = s(z)$ during training and reveals three qualitative regimes. CalAttn first recovers a near-global rescaling and then learns representation-conditioned deviations correlate with improved calibration.

Phase I — global alignment (epochs 0–30). The mean $s(z)$ rapidly decreases while the coefficient of variation CV_s drops, suggesting that CalAttn first behaves similarly to a near-global temperature rescaling.

Phase II — near-uniform modulation (epochs 30–150). After the first learning-rate decay, CV_s remains low and most samples receive similar scales, indicating limited instance-wise differentiation at this stage.

Phase III — heteroscedastic modulation (epochs 150–350). As training progresses, CV_s increases and CalAttn assigns more diverse scales across samples. Meanwhile, the mean scale crosses $s = 1$, transitioning from cooling ($s > 1$) to sharpening ($s < 1$). This coincides with improved calibration, consistent with the hypothesis that representation-conditioned scaling becomes more expressive late in training.

3.5 Reliability Diagrams

Figures 5 present reliability diagrams before any post-hoc temperature scaling. For all three backbones, the vanilla models display pronounced deviations from the diagonal in the high-confidence regime, indicating systematic overconfidence. In contrast, incorporating CalAttn substantially reduces these deviations, producing curves that more closely follow the identity line.

3.6 Robustness under Distribution Shift

Table 4 reports AUROC for detecting distribution shift from CIFAR-10 to SVHN and CIFAR-10-C. CalAttn improves OoD detection in most settings, with larger gains under corruption shift (CIFAR-10-C) than cross-dataset transfer (SVHN). This pattern is consistent with the intuition that corruption shifts preserve more of the ID representation geometry, whereas severe domain shifts may alter features in ways that reduce the reliability of confidence modulation.

3.7 Ablations: inputs and head variants

We ablate the representation used to predict the temperature while keeping training settings fixed: (i) **CLS** (default), (ii) **Patch-Mean** (mean pooling of patch tokens), and (iii) **Concat** (CLS concatenated with Patch-Mean). Table 5 shows that Patch-Mean can improve calibration for ViT/DeiT, while CLS remains competitive for Swin, suggesting that the optimal uncertainty cue depends on how a backbone aggregates global information. We also compare a scalar temperature head against a more expressive Dirichlet α -head (Table 6). The scalar head achieves better calibration with fewer parameters, supporting the choice of rank-preserving temperature scaling as a stable and lightweight design.

Table 5: **Ablation on CalAttn input features.** Three feature choices for predicting the per-sample temperature.

| Dataset | Backbone | Feature | ECE | AdaECE | smECE |
|-----------|----------|------------|-------------|-------------|-------------|
| CIFAR-100 | DeiT-S | CLS | 6.87 | 6.87 | 6.87 |
| | | Patch-Mean | 4.38 | 4.41 | 4.38 |
| | | Concat | 7.29 | 7.29 | 7.28 |
| | ViT-224 | CLS | 4.76 | 8.25 | 8.24 |
| | | Patch-Mean | 2.46 | 2.18 | 2.32 |
| | | Concat | 11.56 | 11.56 | 11.55 |
| | Swin-S | CLS | 1.93 | 2.20 | 1.99 |
| | | Patch-Mean | 4.43 | 4.46 | 4.40 |
| | | Concat | 3.02 | 3.07 | 3.03 |
| CIFAR-10 | DeiT-S | CLS | 4.10 | 4.08 | 4.07 |
| | | Patch-Mean | 4.89 | 4.87 | 4.85 |
| | | Concat | 4.20 | 4.21 | 4.21 |
| | ViT-224 | CLS | 4.76 | 4.47 | 4.75 |
| | | Patch-Mean | 5.82 | 5.82 | 5.82 |
| | | Concat | 5.54 | 5.52 | 4.26 |
| | Swin-S | CLS | 1.74 | 1.66 | 1.63 |
| | | Patch-Mean | 1.78 | 1.90 | 1.78 |
| | | Concat | 1.25 | 1.39 | 1.36 |

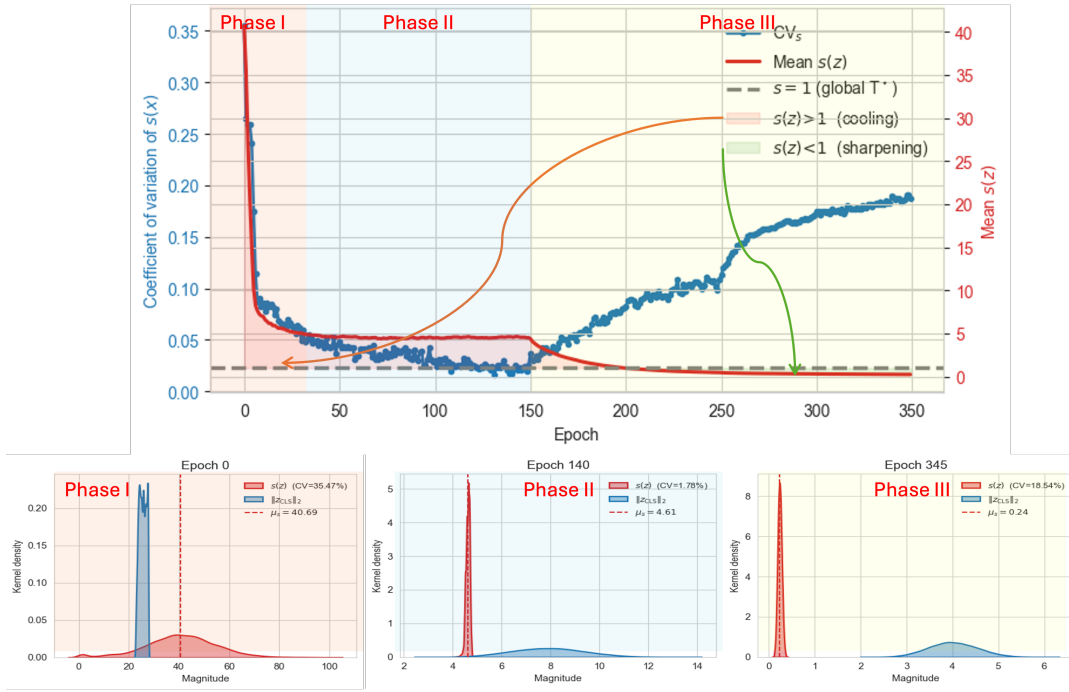


Figure 4: **Temporal dynamics of CalAttn on ViT-224 (CIFAR-10).** *Top*: mean effective temperature $\tau(x) = 1/s(x)$ (red) and its coefficient of variation CV_τ (blue) over training. The dashed line marks the optimal *global* temperature T^* obtained by post-hoc temperature scaling. *Bottom*: kernel density estimates of $\tau(x)$ and $\|z_{CLS}\|_2$ at three epochs.

Table 4: OOD robustness measured by AUROC (%) \uparrow for detecting distribution shift from CIFAR-10 (ID) to SVHN and CIFAR-10-C.

| Dataset | Model | WD [Guo <i>et al.</i> , 2017] | Brier [Brier, 1950] | MMCE [Kumar <i>et al.</i> , 2018] | LabelSmooth [Szegedy <i>et al.</i> , 2016] | Focal [Mukhoti <i>et al.</i> , 2020a] | DualFocal [Tao <i>et al.</i> , 2023] |
|-------------------------|-----------------|-------------------------------|---------------------|-----------------------------------|--------------------------------------------|---------------------------------------|--------------------------------------|
| C10 \rightarrow SVHN | ViT-224 | 70.03 | 61.11 | 69.32 | 68.75 | 67.43 | 70.24 |
| | ViT-224+CalAttn | 74.48 | 63.03 | 69.56 | 68.82 | 70.11 | 75.36 |
| | DeiT-S | 72.40 | 57.21 | 70.31 | 67.24 | 66.38 | 69.09 |
| | DeiT-S+CalAttn | 73.72 | 63.74 | 74.53 | 74.06 | 70.43 | 76.93 |
| | Swin-S | 69.42 | 68.53 | 66.16 | 75.46 | 60.98 | 70.07 |
| | Swin-S+CalAttn | 70.43 | 52.34 | 72.45 | 78.92 | 67.67 | 72.12 |
| C10 \rightarrow C10-C | ViT-224 | 52.86 | 52.19 | 52.85 | 51.53 | 52.33 | 51.71 |
| | ViT-224+CalAttn | 62.40 | 63.35 | 62.60 | 61.08 | 62.34 | 63.21 |
| | DeiT-S | 52.19 | 51.93 | 52.61 | 51.80 | 52.47 | 52.35 |
| | DeiT-S+CalAttn | 61.50 | 63.86 | 62.34 | 59.01 | 58.27 | 60.27 |
| | Swin-S | 59.71 | 54.60 | 67.48 | 61.57 | 60.68 | 58.59 |
| | Swin-S+CalAttn | 61.69 | 57.84 | 59.25 | 64.81 | 69.61 | 63.75 |

Table 6: **Scalar temperature vs. Dirichlet α -head** on CIFAR-100 (ViT-224). Lower is better for calibration metrics.

| Head | Top-1 \uparrow | ECE \downarrow | AdaECE \downarrow | NLL \downarrow | Params \downarrow |
|--------------------|------------------|------------------|---------------------|------------------|---------------------|
| Scalar (ours) | 66.25 | 2.46 | 2.18 | 2.72 | +0.07% |
| Dirichlet α | 64.97 | 7.33 | 7.33 | 2.89 | +0.21% |

3.8 ImageNet-1K results

We evaluate CalAttn on ImageNet-1K using Swin-S (Table 7). CalAttn reduces ECE and AdaECE while maintaining Top-1 accuracy within a narrow range of competitive baselines. We also compare to SATS [Joy *et al.*, 2023] under the same post-hoc TS protocol (Table 8). While SATS performs post-hoc regression on frozen outputs, CalAttn learns representation-conditioned temperatures jointly with the backbone, yielding a different inductive bias. Appendix H provides a conceptual comparison.

Table 7: **ImageNet-1K calibration on Swin-S** under 350 epochs.

| Method | Top-1 \uparrow | ECE \downarrow | AdaECE ⁴ \downarrow |
|---------------------------------------------|------------------|------------------|----------------------------------|
| CE [Guo <i>et al.</i> , 2017] | 75.60 | 9.95 | 9.94 |
| CE+BS [Brier, 1950] | 76.80 | 4.95 | 5.42 |
| MBLS [Liu <i>et al.</i> , 2022] | 77.18 | 1.95 | 1.73 |
| CSM [Luo <i>et al.</i> , 2025] ³ | 81.08 | 1.49 | 1.86 |
| CE+BS+CalAttn (Ours) | 79.68 | 1.25 | 1.43 |

³CSM uses extra re-annotation and curriculum strategies.

⁴Adaptive Expected Calibration Error (AdaECE) [Ding *et al.*, 2020] mitigates bias by adaptive-width bins with equal samples.

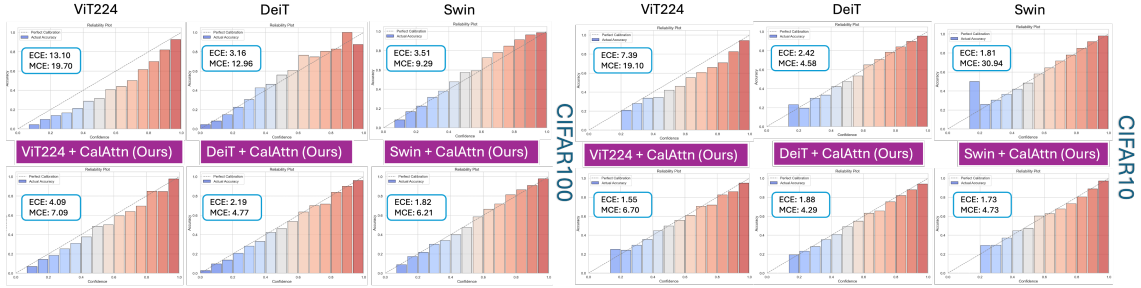


Figure 5: Reliability diagrams before temperature scaling (CIFAR-10/100, 300 epochs).

Table 8: SATS vs. CalAttn on CIFAR-10/100 and Tiny-ImageNet with post-hoc temperature scaling.

| Dataset | Model | Method | ECE | AdaECE |
|---------------|-----------|---------|-------------|-------------|
| CIFAR-10 | WRN-28-10 | SATS | 1.65 | 1.61 |
| | | SATS | 1.61 | 1.53 |
| | ViT-224 | CalAttn | 1.21 | 1.86 |
| | DeiT-S | CalAttn | 1.22 | 1.39 |
| | Swin-S | CalAttn | 0.94 | 0.88 |
| CIFAR-100 | WRN-28-10 | SATS | 3.67 | 3.64 |
| | | SATS | 3.30 | 3.32 |
| | ViT-224 | CalAttn | 1.49 | 1.47 |
| | DeiT-S | CalAttn | 0.86 | 1.73 |
| | Swin-S | CalAttn | 1.51 | 1.75 |
| Tiny-ImageNet | WRN-28-10 | SATS | 4.43 | 4.21 |
| | | SATS | 2.71 | 2.60 |
| | ViT-224 | CalAttn | 0.78 | 0.75 |
| | DeiT-S | CalAttn | 0.83 | 0.52 |
| | Swin-S | CalAttn | 0.24 | 0.46 |

4 Discussion

4.1 Interpreting the gains of CalAttn

From latent uncertainty cues to actionable confidence modulation. CalAttn improves multiple calibration criteria (Tables 1 and Appendix tables), and reliability diagrams (Fig. 5) show that the largest corrections occur in the high-confidence regime where over-confidence is most harmful. Operationally, CalAttn cools over-confident predictions ($s > 1$) and sharpens under-confident ones ($s < 1$), producing reliability curves closer to the identity line.

A heteroscedastic view. The results support a heteroscedastic interpretation: the [CLS] embedding encodes sample-dependent uncertainty cues, and CalAttn learns a nonlinear mapping from representation to an instance-wise temperature. The temporal analysis (Fig. 4) suggests that CalAttn first behaves similarly to a near-global temperature and later increases instance-wise diversity, consistent with calibration improvements that emerge as training converges.

Adaptivity matters beyond architecture. After applying a single global temperature T^* , the calibration gap between architectures narrows, but representation-conditioned scaling reintroduces a clear advantage by enabling sample-specific modulation. This indicates that adaptivity in confidence adjustment can be a key factor in reducing over-confidence be-

yond what a global post-hoc transform can achieve.

4.2 Limitations and extensions

CalAttn predicts a per-sample *scalar* temperature, which preserves logit ordering at inference and therefore does not change top-1 decisions given fixed logits. This design is lightweight and stable, but it cannot express class-conditional or vector/matrix rescaling. Extending CalAttn to classwise temperatures, low-rank scaling, or structured Dirichlet-style parameterizations is a natural direction, trading off expressiveness against parameter count and optimization stability.

5 Related Work

Vision Transformers. Vision Transformers (ViT) [Dosovitskiy *et al.*, 2021] showed that Transformer encoders can achieve competitive image classification performance. DeiT [Touvron *et al.*, 2021] improved data efficiency via distillation, while Swin [Liu *et al.*, 2021] introduced hierarchical windowed attention. Despite architectural refinements [Yuan *et al.*, 2021; Chen *et al.*, 2021; Dai *et al.*, 2021], most models retain a standard linear classification head and rely on external procedures for calibration. **Calibration in classification.** Post-hoc calibration includes Platt scaling and temperature scaling [Platt and others, 1999; Guo *et al.*, 2017], as well as more flexible variants such as vector or matrix scaling. Training-time methods include label smoothing [Müller *et al.*, 2019], focal-style objectives [Mukhoti *et al.*, 2020a; Tao *et al.*, 2023; Liang *et al.*, 2024a], and differentiable surrogates of calibration error. Bayesian and ensemble-based approaches often improve uncertainty estimates but typically incur substantial computational overhead [Gal and Ghahramani, 2016; Lakshminarayanan *et al.*, 2017; Ovadia *et al.*, 2019]. **Sample-wise temperature scaling.** Several works predict sample-dependent temperatures using intermediate features or auxiliary predictors (e.g., Relaxed Softmax [Neumann *et al.*, 2018], Joy *et al.* [Joy *et al.*, 2023]).

6 Conclusion

We study *representation-conditioned* calibration, where confidence is modeled as a function of internal features. In contrast to logit-only calibrators that estimate a global or sample-dependent temperature from the output layer, CalAttn predicts a strictly positive scale from the final transformer representation and applies it as a ranking-preserving modulation.

References

- [Błasiok and Nakkiran, 2023] Jarosław Błasiok and Preetum Nakkiran. Smooth ece: Principled reliability diagrams via kernel smoothing. *arXiv preprint arXiv:2309.12236*, 2023.
- [Brier, 1950] Glenn W. Brier. Verification of forecasts expressed in terms of probability. *Monthly weather review*, 78(1):1–3, 1950.
- [Błasiok, Jarosław and Nakkiran, Preetum, 2024] Błasiok, Jarosław and Nakkiran, Preetum. ml-calibration. <https://github.com/apple/ml-calibration>, 2024. Accessed: 2024-10-08.
- [Chen *et al.*, 2021] Zhengsu Chen, Lingxi Xie, Jianwei Niu, Xuefeng Liu, Longhui Wei, and Qi Tian. Visformer: The vision-friendly transformer. In *Proceedings of the IEEE/CVF international conference on computer vision*, pages 589–598, 2021.
- [Dai *et al.*, 2021] Zihang Dai, Hanxiao Liu, Quoc V Le, and Mingxing Tan. Coatnet: Marrying convolution and attention for all data sizes. *Advances in neural information processing systems*, 34:3965–3977, 2021.
- [Ding *et al.*, 2020] Yukun Ding, Jinglan Liu, Jinjun Xiong, and Yiyu Shi. Revisiting the Evaluation of Uncertainty Estimation and Its Application to Explore Model Complexity-Uncertainty Trade-Off. In *2020 IEEE/CVF Conference on Computer Vision and Pattern Recognition Workshops (CVPRW)*, pages 22–31, Los Alamitos, CA, USA, June 2020. IEEE Computer Society.
- [Dosovitskiy *et al.*, 2021] Alexey Dosovitskiy, Lucas Beyer, Alexander Kolesnikov, Dirk Weissenborn, Xiaohua Zhai, Thomas Unterthiner, Mostafa Dehghani, Matthias Minderer, Georg Heigold, Sylvain Gelly, Jakob Uszkoreit, and Neil Houlsby. An image is worth 16x16 words: Transformers for image recognition at scale. In *International Conference on Learning Representations (ICLR)*, 2021.
- [Feng *et al.*, 2021] Di Feng, Ali Harakeh, Steven L Waslander, and Klaus Dietmayer. A review and comparative study on probabilistic object detection in autonomous driving. *IEEE Transactions on Intelligent Transportation Systems*, 23(8):9961–9980, 2021.
- [Gal and Ghahramani, 2016] Yarin Gal and Zoubin Ghahramani. Dropout as a bayesian approximation: Representing model uncertainty in deep learning. In *international conference on machine learning*, pages 1050–1059. PMLR, 2016.
- [Guo *et al.*, 2017] Chuan Guo, Geoff Pleiss, Yu Sun, and Kilian Q Weinberger. On calibration of modern neural networks. In *International Conference on Machine Learning*, pages 1321–1330. PMLR, 2017.
- [Joy *et al.*, 2023] Tom Joy, Francesco Pinto, Ser-Nam Lim, Philip HS Torr, and Puneet K Dokania. Sample-dependent adaptive temperature scaling for improved calibration. In *Proceedings of the AAAI Conference on Artificial Intelligence*, volume 37, pages 14919–14926, 2023.
- [Kumar *et al.*, 2018] Aviral Kumar, Sunita Sarawagi, and Ujjwal Jain. Trainable calibration measures for neural networks from kernel mean embeddings. In *International Conference on Machine Learning*, pages 2805–2814. PMLR, 2018.
- [Lakshminarayanan *et al.*, 2017] Balaji Lakshminarayanan, Alexander Pritzel, and Charles Blundell. Simple and scalable predictive uncertainty estimation using deep ensembles. *Advances in neural information processing systems*, 30, 2017.
- [Liang *et al.*, 2024a] Wenhao Liang, Chang Dong, Liangwei Zheng, Zhengyang Li, Wei Zhang, and Weitong Chen. Calibrating deep neural network using euclidean distance. *arXiv preprint arXiv:2410.18321*, 2024.
- [Liang *et al.*, 2024b] Wenhao Liang, Zhengyang Li, and Weitong Chen. Enhancing financial market predictions: Causality-driven feature selection. In *Advanced Data Mining and Applications*. Springer, 2024.
- [Liu *et al.*, 2021] Ze Liu, Yutong Lin, Yue Cao, Han Hu, Yixuan Wei, Zheng Zhang, Stephen Lin, and Baining Guo. Swin transformer: Hierarchical vision transformer using shifted windows. In *Proceedings of the IEEE/CVF international conference on computer vision*, pages 10012–10022, 2021.
- [Liu *et al.*, 2022] Bingyuan Liu, Ismail Ben Ayed, Adrian Galdran, and Jose Dolz. The devil is in the margin: Margin-based label smoothing for network calibration. In *Proceedings of the IEEE/CVF Conference on Computer Vision and Pattern Recognition*, pages 80–88, 2022.
- [Luo *et al.*, 2025] Haoyang Luo, Linwei Tao, Minjing Dong, and Chang Xu. Beyond one-hot labels: Semantic mixing for model calibration. *arXiv preprint arXiv:2504.13548*, 2025.
- [Mehrtash *et al.*, 2020] Alireza Mehrtash, William M Wells, Clare M Tempny, Purang Abolmaesumi, and Tina Kapur. Confidence calibration and predictive uncertainty estimation for deep medical image segmentation. *IEEE transactions on medical imaging*, 39(12):3868–3878, 2020.
- [Minderer *et al.*, 2021] Matthias Minderer, Josip Djolonga, Rob Romijnders, Frances Hubis, Xiaohua Zhai, Neil Houlsby, Dustin Tran, and Mario Lucic. Revisiting the calibration of modern neural networks. *Advances in Neural Information Processing Systems*, 34:15682–15694, 2021.
- [Mukhoti *et al.*, 2020a] Jishnu Mukhoti, Viveka Kulharia, Amartya Sanyal, Stuart Golodetz, Philip Torr, and Puneet Dokania. Calibrating deep neural networks using focal loss. *Advances in Neural Information Processing Systems*, 33:15288–15299, 2020.
- [Mukhoti *et al.*, 2020b] Jishnu Mukhoti, Viveka Kulharia, Amartya Sanyal, Stuart Golodetz, Philip HS Torr, and Puneet K Dokania. Focal calibration. https://github.com/torrvision/focal_calibration, 2020. Accessed: 2024-10-08.
- [Müller *et al.*, 2019] Rafael Müller, Simon Kornblith, and Geoffrey E. Hinton. When does label smoothing help? *Advances in neural information processing systems*, 32, 2019.

- [Naseer *et al.*, 2021] Muhammad Muzammal Naseer, Kanchana Ranasinghe, Salman H Khan, Munawar Hayat, Fahad Shahbaz Khan, and Ming-Hsuan Yang. Intriguing properties of vision transformers. *Advances in Neural Information Processing Systems*, 34:23296–23308, 2021.
- [Neumann *et al.*, 2018] Lukas Neumann, Andrew Zisserman, and Andrea Vedaldi. Relaxed softmax: Efficient confidence auto-calibration for safe pedestrian detection. 2018.
- [Ovadia *et al.*, 2019] Yaniv Ovadia, Emily Fertig, Jie Ren, Zachary Nado, David Sculley, Sebastian Nowozin, Joshua Dillon, Balaji Lakshminarayanan, and Jasper Snoek. Can you trust your model’s uncertainty? evaluating predictive uncertainty under dataset shift. *Advances in neural information processing systems*, 32, 2019.
- [Platt and others, 1999] John Platt et al. Probabilistic outputs for support vector machines and comparisons to regularized likelihood methods. *Advances in large margin classifiers*, 10(3):61–74, 1999.
- [Szegedy *et al.*, 2016] Christian Szegedy, Vincent Vanhoucke, Sergey Ioffe, Jon Shlens, and Zbigniew Wojna. Rethinking the inception architecture for computer vision. In *cvpr*, 2016.
- [Tao *et al.*, 2023] Linwei Tao, Minjing Dong, and Chang Xu. Dual focal loss for calibration. In *International Conference on Machine Learning (ICML)*, 2023.
- [Touvron *et al.*, 2021] Hugo Touvron, Matthieu Cord, Matthijs Douze, Francisco Massa, Alexandre Sablayrolles, and Hervé Jégou. Training data-efficient image transformers & distillation through attention. In *International Conference on Machine Learning*, pages 10347–10357. PMLR, 2021.
- [Yuan *et al.*, 2021] Li Yuan, Yunpeng Chen, Tao Wang, Weihao Yu, Yujun Shi, Zi-Hang Jiang, Francis EH Tay, Jiashi Feng, and Shuicheng Yan. Tokens-to-token vit: Training vision transformers from scratch on imagenet. In *Proceedings of the IEEE/CVF international conference on computer vision*, pages 558–567, 2021.
- [Zhou *et al.*, 2022] Daquan Zhou, Zhiding Yu, Enze Xie, Chaowei Xiao, Animashree Anandkumar, Jiashi Feng, and Jose M Alvarez. Understanding the robustness in vision transformers. In *International conference on machine learning*, pages 27378–27394. PMLR, 2022.

APPENDIX

A Notation for Calibration Attention

Table 9 and Table 10 summarize the symbols used in the paper. Shapes correspond to vision classification unless otherwise specified.

Table 9: Notation for CalAttn (model and training).

| Symbol | Description | Shape / Type |
|----------------------------------|-----------------------------------------------------------------|-------------------|
| B | batch size | scalar |
| C | number of classes | scalar |
| d | [CLS] embedding dim. | 384 / 768 |
| H, W | input height / width | e.g. 32, 224 |
| \mathbf{x} | input image | $(B, 3, H, W)$ |
| \mathbf{z}_{CLS} | final [CLS] embedding | (B, d) |
| $W_{\text{cls}}, b_{\text{cls}}$ | classifier parameters | $(C, d), (C)$ |
| ℓ | logits $W_{\text{cls}}\mathbf{z}_{\text{CLS}} + b_{\text{cls}}$ | (B, C) |
| $\hat{\mathbf{y}}$ | probs. softmax(ℓ) | (B, C) |
| h | CalAttn hidden width | 128 |
| W_1 | CalAttn first-layer weight | (h, d) |
| \mathbf{w}_2, b_2 | CalAttn second-layer weight/bias | $(h), ()$ |
| \mathbf{h} | GELU($W_1\mathbf{z}_{\text{CLS}}$) | (B, h) |
| $s(\mathbf{z})$ | predicted scale (> 0) | $(B, 1)$ |
| ε | numerical constant | 10^{-6} |
| $\tilde{\ell}$ | scaled logits $\ell/s(\mathbf{z})$ | (B, C) |
| $\hat{\mathbf{y}}$ | calibrated probs. softmax($\tilde{\ell}$) | (B, C) |
| y | ground-truth label | $\{1, \dots, C\}$ |
| \mathbf{e}_y | one-hot label vector | (B, C) |
| λ | Brier weight | scalar |

B Calibration Metrics

A model is perfectly calibrated if $\Pr(y = \hat{y} \mid \hat{p} = p) = p$ for all $p \in [0, 1]$.

ECE / MCE / AdaECE / ClassECE. Let $\hat{p}_i = \max_c \hat{y}_{ic}$ and partition $[0, 1]$ into M bins $\{B_m\}_{m=1}^M$. Define

$$\text{acc}(B_m) = \frac{1}{|B_m|} \sum_{i \in B_m} \mathbb{1}(\hat{y}_i = y_i), \quad (6)$$

$$\text{conf}(B_m) = \frac{1}{|B_m|} \sum_{i \in B_m} \hat{p}_i. \quad (7)$$

Then

$$\text{ECE} = \sum_{m=1}^M \frac{|B_m|}{N} |\text{acc}(B_m) - \text{conf}(B_m)|, \quad (8)$$

$$\text{MCE} = \max_m |\text{acc}(B_m) - \text{conf}(B_m)|. \quad (9)$$

AdaECE uses *adaptive* bins $\{B_m^{\text{ad}}\}_{m=1}^M$ constructed such that $|B_m^{\text{ad}}| \approx N/M$:

$$\text{AdaECE} = \sum_{m=1}^M \frac{|B_m^{\text{ad}}|}{N} |\text{acc}(B_m^{\text{ad}}) - \text{conf}(B_m^{\text{ad}})|. \quad (10)$$

Table 10: Notation for calibration metrics.

| Symbol | Description | Shape / Type |
|-----------------------------|--------------------------------------|--------------|
| N | number of evaluation samples | scalar |
| M | number of bins | scalar |
| \hat{p}_i | max confidence $\max_c \hat{y}_{ic}$ | scalar |
| B_m | fixed-width ECE bin m | index set |
| B_m^{ad} | adaptive (equal-count) bin m | index set |
| $B_{m,c}$ | class- c bin m (ClassECE) | index set |
| $\text{acc}(\cdot)$ | bin accuracy | scalar |
| $\text{conf}(\cdot)$ | bin confidence | scalar |
| ECE / MCE | calibration metrics | scalar |
| / AdaECE / ClassECE / smECE | | |

ClassECE averages class-conditional ECE over classes. For each class c , let $\hat{p}_i^{(c)} = \hat{y}_{ic}$ and bin predictions for class c to obtain $\{B_{m,c}\}_{m=1}^M$. Then

$$\text{ClassECE} = \frac{1}{C} \sum_{c=1}^C \sum_{m=1}^M \frac{|B_{m,c}|}{N} |\text{acc}(B_{m,c}) - \text{conf}(B_{m,c})|. \quad (11)$$

Smooth ECE (smECE). [Błasiok and Nakkiran, 2023] replace bins with Gaussian kernels:

$$\widehat{\text{acc}}(\hat{p}_i) = \frac{\sum_j K_h(\hat{p}_i - \hat{p}_j) \mathbb{1}(\hat{y}_j = y_j)}{\sum_j K_h(\hat{p}_i - \hat{p}_j)}, \quad (12)$$

$$\text{smECE} = \frac{1}{N} \sum_i |\widehat{\text{acc}}(\hat{p}_i) - \hat{p}_i|. \quad (13)$$

We fix $h = 0.05$.

Usage in this work. We report all metrics above and show that CalAttn consistently reduces each, confirming improvements beyond histogram artefacts.

C Vision Transformer with Calibration Attention: Forward Pass

Patch embedding. Given an input image $\mathbf{x} \in \mathbb{R}^{3 \times H \times W}$, a convolutional projection with kernel and stride P maps the image to a sequence of patch tokens:

$$\mathbf{X}_{\text{patch}} = \text{reshape}(\text{Conv}_{3 \rightarrow D}^{P \times P}(\mathbf{x}), N, D) \in \mathbb{R}^{N \times D}, \quad N = \frac{HW}{P^2}.$$

Class token and positional encoding. A learned class token $\mathbf{z}_{\text{CLS}} \in \mathbb{R}^{1 \times D}$ is prepended and positional embeddings are added:

$$\mathbf{z}^{(0)} = [\mathbf{z}_{\text{CLS}}; \mathbf{X}_{\text{patch}}] + \mathbf{E}_{\text{pos}} \in \mathbb{R}^{(N+1) \times D}.$$

Transformer encoder blocks. For layers $\ell = 1, \dots, L$, with pre-norm residual blocks:

$$\begin{aligned} \mathbf{u}^{(\ell)} &= \text{LN}(\mathbf{z}^{(\ell-1)}), \\ \mathbf{z}^{(\ell)} &= \mathbf{z}^{(\ell-1)} + \text{MSA}(\mathbf{u}^{(\ell)}), \\ \mathbf{v}^{(\ell)} &= \text{LN}(\mathbf{z}^{(\ell)}), \\ \mathbf{z}^{(\ell)} &= \mathbf{z}^{(\ell)} + \text{MLP}(\mathbf{v}^{(\ell)}). \end{aligned}$$

Calibration Attention head. Let $\mathbf{z}_{\text{CLS}} = \mathbf{z}_0^{(L)} \in \mathbb{R}^D$ denote the final [CLS] token (the first token of $\mathbf{z}^{(L)}$). CalAttn predicts a strictly positive scale

$$s(\mathbf{x}) = \text{Softplus}(\mathbf{w}_2^\top \text{GELU}(\mathbf{W}_1 \mathbf{z}_{\text{CLS}}) + b_2) + \varepsilon,$$

where $\mathbf{W}_1 \in \mathbb{R}^{h \times D}$, $\mathbf{w}_2 \in \mathbb{R}^h$, $b_2 \in \mathbb{R}$, and $\varepsilon > 0$.

Calibrated prediction. A linear classifier produces logits $\ell = W_{\text{cls}} \mathbf{z}_{\text{CLS}} + b_{\text{cls}} \in \mathbb{R}^C$. CalAttn rescales logits and outputs calibrated probabilities:

$$\tilde{\ell} = \ell / s(\mathbf{x}), \quad \hat{\mathbf{y}} = \text{softmax}(\tilde{\ell}).$$

Training objective. We train end-to-end with a proper scoring objective:

$$\mathcal{L} = \mathcal{L}_{\text{CE}}(\hat{\mathbf{y}}, y) + \lambda \|\hat{\mathbf{y}} - \mathbf{e}_y\|_2^2, \quad \lambda = 0.1.$$

D Architectural Differences

Table 11 contrasts a vanilla ViT with ViT equipped with Calibration Attention (CalAttn).

E Why the Learned Scale Approximates the Conditional Optimal Temperature

Let $\ell(x) \in \mathbb{R}^C$ denote the logits produced by a fixed classifier for input x , and let $s(x) > 0$ be the CalAttn scale. Define scaled logits $\tilde{\ell}(x) = \ell(x)/s(x)$ and the predictive distribution $\hat{\mathbf{y}}(x, s) = \text{softmax}(\tilde{\ell}(x))$. The per-sample training loss is

$$\mathcal{L}(x, y; s) = -\log \hat{y}_y(x, s) + \lambda \|\hat{\mathbf{y}}(x, s) - \mathbf{e}_y\|_2^2. \quad (14)$$

Proper scoring perspective. For a fixed input x , consider the conditional risk

$$\mathcal{R}_x(s) = \mathbb{E}_{y \sim p(y|x)} [\mathcal{L}(x, y; s)].$$

Both the cross-entropy and the Brier score are strictly proper scoring rules, and any nonnegative weighted sum of strictly proper scoring rules is strictly proper. Therefore, viewed as a function of the predicted distribution $\hat{\mathbf{y}}$, the conditional risk is uniquely minimized at the true posterior:

$$\arg \min_{\hat{\mathbf{y}} \in \Delta^{C-1}} \mathbb{E}_{y \sim p(y|x)} [-\log \hat{y}_y + \lambda \|\hat{\mathbf{y}} - \mathbf{e}_y\|_2^2] = p(y | x).$$

This identifies the *target* distribution that the calibration head should produce.

From distributions to a scalar scale. CalAttn does not predict an arbitrary distribution; it predicts a *scalar* $s(x)$ that modulates sharpness while preserving the logit ordering. Hence the best achievable predictor under CalAttn belongs to the one-parameter family

$$\mathcal{F}_x = \left\{ \text{softmax}(\ell(x)/s) : s > 0 \right\}.$$

Define the *CalAttn-optimal* conditional scale as

$$s^*(x) \in \arg \min_{s > 0} \mathcal{R}_x(s).$$

When the true posterior is representable by temperature scaling, i.e., when there exists an $s > 0$ such that $p(y | x) = \text{softmax}(\ell(x)/s)$, any minimizer $s^*(x)$ satisfies

$$\hat{\mathbf{y}}(x, s^*(x)) = p(y | x). \quad (15)$$

In general, if $p(y | x) \notin \mathcal{F}_x$, then $s^*(x)$ yields the best approximation to $p(y | x)$ within \mathcal{F}_x under the strictly proper conditional risk.

Learning with a representation-conditioned head. In practice, $p(y | x)$ is unknown and $s(x)$ is parameterized by a calibration head conditioned on the [CLS] representation, $s(x) = s_\phi(z(x))$. Training minimizes the empirical risk, so the learned head approximates the population minimizer $s^*(x)$ induced by the current representation. This is the sense in which CalAttn learns a representation-conditioned approximation to the conditional optimal temperature.

Proposition (Conditional optimality with frozen logits).

Fix logits $\ell(x)$ (equivalently, freeze backbone and classifier). Assume $p(y | x)$ is well-defined for each x and $\lambda \geq 0$. Let $\hat{\mathbf{y}}(x, s) = \text{softmax}(\ell(x)/s)$. Then any minimizer $s^*(x) \in \arg \min_{s > 0} \mathcal{R}_x(s)$ produces the best CalAttn-representable calibrated distribution for that x , and if $p(y | x) \in \mathcal{F}_x$ then Eq. (15) holds.

Remark (Scope). The statement is conditional on fixed logits (or frozen backbone parameters). It does not assert global optimality for joint training over the backbone and the calibration head. Rather, it formalizes the calibration head’s role: given a representation/logit geometry, optimizing s_ϕ moves predictions toward the conditional optimum achievable by temperature scaling.

F smECE, AdaECE and Classwise-ECE

We further report Smooth ECE (smECE), Adaptive ECE (AdaECE) and Classwise-ECE in Tables 12, 17 and 18. Their reduction of relative changes are reported in Fig. 6 and Fig. 7. Following standard practice, we use SGD for CNN backbones and AdamW ($\beta = (0.9, 0.999)$, weight decay 0.05) for Transformer backbones (ViT, DeiT, Swin) with cosine learning-rate scheduling. To ensure that the observed calibration improvements are not artifacts of the optimizer choice, we additionally retrain each backbone using the alternative optimizer and evaluate CE, post-hoc TS, and CalAttn under identical settings. The relative ordering of methods remains unchanged, confirming that the gains of CalAttn are robust to optimizer variation.

G Impact of Calibration on Model Size

Computational and parameter overhead. CalAttn adds a two-layer MLP that maps the final [CLS] embedding of dimension d to a scalar scale using hidden width h . The additional parameter count is

$$\underbrace{hd}_{W_1} + \underbrace{h}_{b_1} + \underbrace{h}_{w_2} + \underbrace{1}_{b_2} = O(dh),$$

and the extra per-sample compute is dominated by two matrix-vector products, i.e., $O(dh)$ FLOPs, plus a scalar division. This overhead is negligible relative to a Transformer encoder, whose attention and MLP blocks scale on the order of $O(LNd^2)$ with depth L and token count N .

⁴Smooth ECE (smECE) is introduced by [Błasiok and Nakkiran, 2023]. We use the authors’ public implementation [Błasiok, Jarosław and Nakkiran, Preetum, 2024] with bandwidth $h = 0.05$.

Table 11: Comparison between a vanilla Vision Transformer and ViT equipped with Calibration Attention (CalAttn).

| Component | Vanilla ViT | ViT + CalAttn (Ours) |
|------------------------------|--------------------------------------------|--------------------------------------------------------------------------------------------------------------------------------------------------------------------|
| Additional module | None | Temperature head: lightweight two-layer MLP applied to the final [CLS] embedding |
| Module output | — | Strictly positive, instance-wise scale $s(\mathbf{z}_{\text{CLS}})$, identity-initialized so that $s(\mathbf{z}_{\text{CLS}}) \approx 1$ at the start of training |
| Logits before softmax | ℓ | $\tilde{\ell} = \ell/s(\mathbf{z}_{\text{CLS}})$, enabling per-sample cooling ($s > 1$) or sharpening ($s < 1$) while preserving logit ordering |
| Training objective | Cross-entropy (CE) | Proper scoring objective: CE + λ Brier (Eq. (3)) |
| Post-hoc temperature scaling | Often applied as a separate post-hoc stage | Optional; CalAttn learns instance-wise scaling during training and can be combined with global TS if desired |
| Parameter overhead | 0 | < 0.1% of backbone parameters (two small fully connected layers) |

Table 12: \downarrow smECE (%) before and after applying global temperature scaling. For each Post-T entry, parentheses report the learned temperature T^* . We select T^* by minimizing validation ECE with 15 equal-width bins ⁴.

| Dataset | Model | Weight Decay [Guo <i>et al.</i> , 2017] | | Brier Loss [Brier, 1950] | | MMCE [Kumar <i>et al.</i> , 2018] | | Label Smooth [Szegedy <i>et al.</i> , 2016] | | Focal Loss - 53 [Mukhoti <i>et al.</i> , 2020a] | | Dual Focal [Tao <i>et al.</i> , 2023] | | CE + λ BS ($\lambda = 0.1$) | |
|---------------|--------------------------------------|-----------------------------------------|-------------------|--------------------------|-------------------|-----------------------------------|-------------------|---------------------------------------------|-------------------|-------------------------------------------------|-------------------|---------------------------------------|-------------------|---------------------------------------|-------------------|
| | | Pre T | Post-T (T^*) | Pre T | Post-T (T^*) | Pre T | Post-T (T^*) | Pre T | Post-T (T^*) | Pre T | Post-T (T^*) | Pre T | Post-T (T^*) | Pre T | Post-T (T^*) |
| CIFAR-100 | ResNet-50 | 14.95 | 2.63(2.20) | 5.34 | 3.53(1.10) | 13.40 | 3.12(1.90) | 6.31 | 3.43(1.10) | 5.56 | 2.37(1.10) | 8.82 | 2.24(1.30) | 13.99 | 2.31(1.60) |
| | ResNet-110 | 15.05 | 3.84(2.30) | 6.53 | 3.51(1.20) | 14.86 | 3.51(2.30) | 9.55 | 4.36(1.30) | 10.98 | 3.60(1.30) | 11.69 | 3.31(1.30) | 17.84 | 3.16(1.80) |
| | Wide-ResNet-26-10 | 12.97 | 2.85(2.10) | 4.06 | 2.78(1.10) | 12.27 | 3.85(2.00) | 3.04 | 3.04(1.00) | 2.84 | 2.20(1.10) | 6.01 | 2.41(0.90) | 6.45 | 5.12(1.20) |
| | DenseNet-121 | 15.42 | 2.61(2.20) | 3.66 | 1.83(1.10) | 15.96 | 2.95(2.00) | 3.85 | 3.68(1.10) | 3.04 | 1.50(1.10) | 4.07 | 1.72(0.90) | 15.75 | 2.83(1.60) |
| | ViT ₂₂₄ | 13.07 | 3.32(1.30) | 2.62 | 2.25(1.10) | 11.51 | 2.25(1.30) | 3.77 | 2.17(1.10) | 5.13 | 3.20(1.10) | 3.43 | 3.43(1.00) | 6.27 | 2.25(1.50) |
| | ViT ₂₂₄ +CalAttn(Ours) | 8.24 | 1.92(1.20) | 1.93 | 2.30(1.00) | 9.04 | 2.16(1.20) | 1.97 | 1.97(1.00) | 2.64 | 2.64(1.00) | 3.66 | 1.96(1.10) | 4.00 | 1.49(1.10) |
| | DeiT _{small} | 7.45 | 3.48(1.10) | 2.13 | 2.13(1.00) | 7.88 | 2.34(1.20) | 1.72 | 1.72(1.00) | 3.01 | 3.01(1.00) | 1.91 | 1.91(1.00) | 5.13 | 2.06(1.40) |
| | DeiT _{small} +CalAttn(Ours) | 6.87 | 1.59(1.20) | 2.13 | 2.05(1.10) | 6.51 | 1.28(1.20) | 1.61 | 1.61(1.00) | 3.08 | 3.08(1.00) | 3.05 | 2.16(1.10) | 4.37 | 1.17(1.10) |
| | Swin _{small} | 3.44 | 2.44(0.90) | 2.55 | 2.55(1.00) | 3.37 | 2.66(0.90) | 8.76 | 2.35(0.80) | 10.55 | 2.42(0.80) | 8.17 | 3.04(0.80) | 3.23 | 2.45(1.20) |
| | Swin _{small} +CalAttn(Ours) | 1.99 | 1.99(1.00) | 3.02 | 1.92(1.10) | 1.76 | 1.76(1.00) | 6.48 | 2.56(0.90) | 5.99 | 2.99(0.90) | 3.76 | 2.92(0.90) | 1.64 | 1.64(1.00) |
| CIFAR-10 | ResNet-50 | 3.27 | 1.48(2.50) | 1.83 | 1.27(1.10) | 3.41 | 1.47(2.60) | 3.31 | 1.92(0.90) | 1.45 | 1.45(1.00) | 1.36 | 1.36(1.00) | 5.18 | 1.67(1.90) |
| | ResNet-110 | 3.43 | 1.88(2.60) | 2.49 | 1.63(1.20) | 3.38 | 1.55(2.80) | 2.87 | 1.52(0.90) | 1.69 | 1.39(1.10) | 1.48 | 1.35(1.10) | 5.28 | 2.25(1.90) |
| | Wide-ResNet-26-10 | 2.70 | 1.25(2.20) | 1.55 | 1.55(1.00) | 3.03 | 1.46(2.20) | 3.75 | 1.47(0.80) | 1.84 | 1.46(0.90) | 3.31 | 1.20(0.80) | 3.41 | 1.64(1.50) |
| | DenseNet-121 | 5.56 | 2.21(2.40) | 3.86 | 1.93(1.10) | 5.86 | 1.95(2.30) | 2.84 | 1.63(0.90) | 3.04 | 1.50(0.90) | 4.07 | 1.72(0.90) | 5.17 | 2.24(1.60) |
| | ViT ₂₂₄ | 7.40 | 1.46(1.30) | 1.89 | 1.89(1.00) | 3.47 | 1.37(1.10) | 1.66 | 1.66(1.00) | 8.53 | 1.97(0.70) | 3.67 | 2.12(0.90) | 4.26 | 3.53(1.40) |
| | ViT ₂₂₄ +CalAttn(Ours) | 4.75 | 1.54(1.20) | 2.56 | 1.86(1.10) | 4.36 | 1.70(1.20) | 2.41 | 1.31(0.90) | 9.95 | 2.06(0.70) | 4.35 | 2.78(0.90) | 1.57 | 1.18(1.10) |
| | DeiT _{small} | 4.41 | 1.56(1.20) | 2.03 | 2.03(1.00) | 6.01 | 1.65(1.20) | 1.64 | 1.64(1.00) | 10.49 | 2.87(0.70) | 5.00 | 2.79(0.80) | 3.85 | 1.96(1.30) |
| | DeiT _{small} +CalAttn(Ours) | 4.07 | 1.76(1.10) | 2.09 | 1.76(1.10) | 3.39 | 1.41(1.10) | 2.15 | 2.15(1.00) | 9.90 | 1.79(0.70) | 3.77 | 2.74(0.90) | 1.89 | 1.36(1.10) |
| | Swin _{small} | 1.43 | 1.93(0.90) | 1.46 | 1.46(1.00) | 1.78 | 2.31(0.90) | 6.68 | 1.36(0.80) | 15.63 | 2.34(0.60) | 8.40 | 2.41(0.70) | 3.11 | 2.04(1.20) |
| | Swin _{small} +CalAttn(Ours) | 1.63 | 1.63(1.00) | 1.19 | 1.19(1.00) | 1.23 | 1.23(1.00) | 5.94 | 1.55(0.80) | 14.94 | 1.61(0.60) | 7.08 | 2.32(0.80) | 1.11 | 1.11(1.00) |
| MNIST | ViT ₂₂₄ | 2.88 | 1.13(0.90) | 39.17 | 3.72(8.70) | 19.77 | 4.89(2.10) | 12.74 | 6.61(1.50) | 7.13 | 2.15(1.40) | 18.28 | 4.52(2.30) | 5.23 | 1.26(0.80) |
| | ViT ₂₂₄ +CalAttn(Ours) | 2.76 | 1.13(0.90) | 3.12 | 1.04(0.90) | 3.89 | 1.41(0.80) | 8.30 | 1.31(0.70) | 23.30 | 1.25(0.40) | 17.99 | 1.45(0.50) | 0.94 | 0.68(0.90) |
| | DeiT _{small} | 2.87 | 1.29(0.90) | 26.66 | 2.53(3.20) | 4.56 | 1.17(0.80) | 8.70 | 1.05(0.70) | 21.32 | 2.39(0.50) | 15.89 | 1.65(0.70) | 4.45 | 1.30(0.80) |
| | DeiT _{small} +CalAttn(Ours) | 1.23 | 1.23(1.00) | 1.17 | 0.68(0.90) | 2.15 | 1.13(0.90) | 6.21 | 1.40(0.80) | 18.17 | 1.56(0.50) | 8.96 | 2.30(0.60) | 1.14 | 1.14(1.00) |
| | Swin _{small} | 3.57 | 3.20(1.10) | 1.28 | 0.71(0.90) | 1.35 | 0.79(0.90) | 8.12 | 0.79(0.70) | 11.77 | 0.96(0.50) | 5.06 | 0.68(0.60) | 0.65 | 0.65(1.00) |
| | Swin _{small} +CalAttn(Ours) | 0.53 | 0.66(1.10) | 0.90 | 0.59(0.90) | 1.22 | 0.68(0.90) | 7.89 | 0.67(0.70) | 7.11 | 0.58(0.50) | 8.81 | 0.66(0.50) | 0.90 | 0.59(0.90) |
| Tiny-ImageNet | ViT ₂₂₄ | 4.39 | 1.80(1.10) | 4.40 | 1.81(1.10) | 4.96 | 1.83(1.20) | 2.20 | 1.65(1.10) | 3.19 | 1.85(1.10) | 2.35 | 2.33(1.10) | 2.45 | 2.41(1.10) |
| | ViT ₂₂₄ +CalAttn(Ours) | 21.61 | 2.88(1.90) | 9.17 | 0.97(1.30) | 19.59 | 2.95(1.80) | 2.00 | 1.59(1.10) | 1.68 | 0.14(1.30) | 13.52 | 1.44(1.40) | 0.89 | 0.89(1.00) |
| | DeiT _{small} | 13.00 | 1.96(1.90) | 2.53 | 1.81(1.10) | 13.61 | 1.16(1.50) | 1.65 | 1.65(1.00) | 10.25 | 2.18(1.70) | 9.36 | 1.90(1.70) | 1.88 | 1.86(1.10) |
| | DeiT _{small} +CalAttn(Ours) | 2.29 | 1.44(1.40) | 2.32 | 1.12(1.20) | 2.72 | 1.45(1.50) | 2.28 | 1.22(1.10) | 2.18 | 1.36(1.30) | 1.90 | 1.19(1.30) | 1.18 | 0.67(1.20) |
| | Swin _{small} | 3.24 | 2.53(0.90) | 0.88 | 0.66(0.90) | 2.04 | 2.04(1.00) | 4.79 | 2.34(0.90) | 4.20 | 2.45(0.90) | 4.64 | 2.46(0.90) | 1.60 | 1.60(1.00) |
| | Swin _{small} +CalAttn(Ours) | 2.88 | 1.32(1.10) | 0.86 | 0.78(1.10) | 1.50 | 1.50(1.00) | 2.51 | 2.51(1.00) | 2.31 | 2.31(1.00) | 2.35 | 2.35(1.00) | 0.92 | 0.64(0.90) |

H Distinguishing CalAttn from SATS

Although both SATS [Joy *et al.*, 2023] and CalAttn predict an instance-wise temperature, they optimize different objectives and intervene at different stages of the model.

Optimization: post-hoc regression vs. end-to-end learning. SATS is a *post-hoc* method: the backbone is frozen and a temperature regressor is fit on a held-out validation set to minimize a calibration criterion (e.g., NLL or ECE):

$$\min_{\phi} \mathbb{E}_{(x,y) \sim \mathcal{D}_{\text{val}}} \mathcal{L} \left(\text{softmax} \left(\frac{\ell(x)}{T_{\phi}(\ell(x))} \right), y \right),$$

where logits $\ell(x)$ are produced by a fixed model.

CalAttn is integrated into training and jointly optimizes the backbone and the scale head under a proper scoring objective:

$$\min_{\theta, \psi} \mathbb{E}_{(x,y) \sim \mathcal{D}} \left[\text{CE} \left(\text{softmax} \left(\frac{\ell_{\theta}(x)}{s_{\psi}(z_{\theta}(x))} \right), y \right) + \lambda \|\hat{\mathbf{y}} - \mathbf{e}_y\|_2^2 \right],$$

where $z_{\theta}(x)$ denotes the final [CLS] embedding and $\hat{\mathbf{y}} = \text{softmax}(\ell_{\theta}(x)/s_{\psi}(z_{\theta}(x)))$.

Conditioning signal: logits vs. representation. SATS conditions temperature on the *logits* via $T_{\phi}(\ell(x))$. Since logits are the output of the classifier head, SATS performs confidence correction *after* the representation and decision boundary have been learned, and it cannot influence feature learning.

In contrast, CalAttn predicts the scale from an *upstream* representation, $s_{\psi}(z_{\theta}(x))$, before the classifier head. Consequently, gradients from the calibration objective backpropagate through $s_{\psi}(\cdot)$ into the [CLS] pathway, enabling representation learning to co-adapt with instance-wise confidence modulation. This distinction provides a different inductive bias from post-hoc regression on frozen outputs and helps explain why CalAttn can remain complementary to global post-hoc temperature scaling.

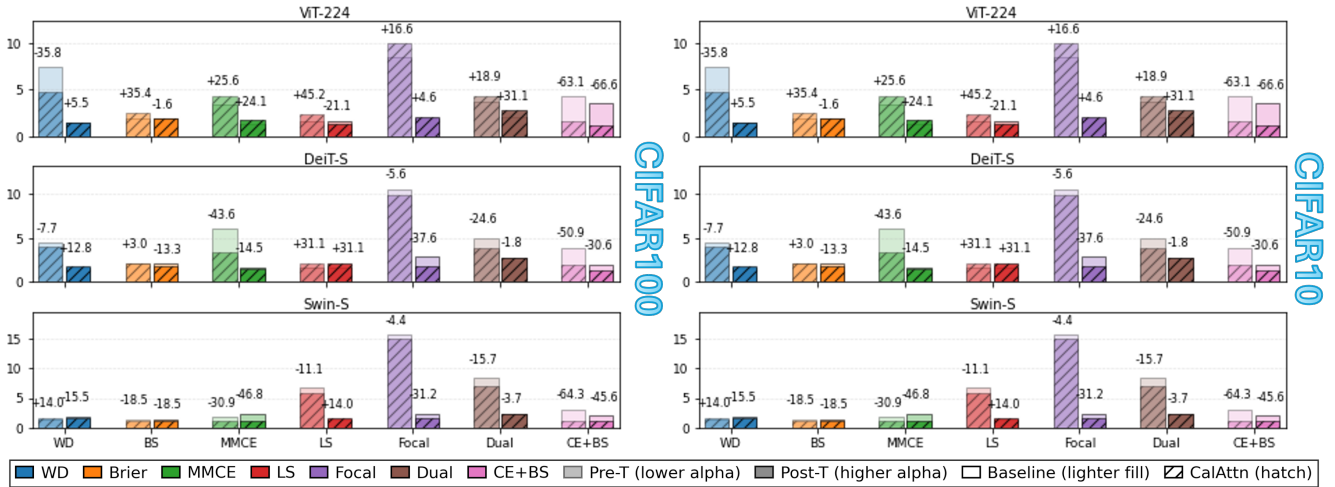


Figure 6: smECE(%) on CIFAR-10/100 across ViT-224, DeiT-S, and Swin-S with relative changes (Δ %, “+” increase, “-” decrease).

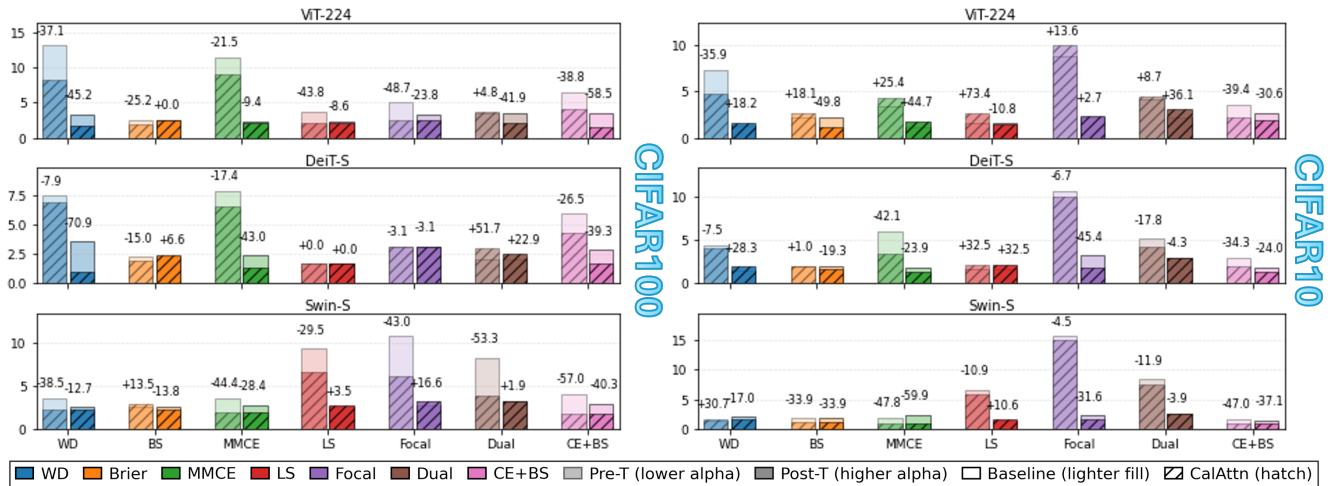


Figure 7: AdaECE(%) on CIFAR-10/100 across ViT-224, DeiT-S, and Swin-S with relative changes (Δ %, “+” increase, “-” decrease).

I Sensitivity to the CE+Brier Trade-off λ (CIFAR-100, DeiT-S)

Unless stated otherwise, all metrics are reported in % and computed *after* applying a single global post-hoc temperature scaling step (TS) to each trained model.

Takeaways. (1) CE+ λ Brier without CalAttn is weakly sensitive to λ . ECE varies by at most 0.11 percentage points over the sweep, indicating a broad plateau.

(2) With CalAttn, performance depends more on λ but remains stable near the default. The best calibration in this sweep occurs at $\lambda = 0.9$; however, $\lambda = 0.1$ remains within 0.6 percentage points in ECE, making it a reasonable default that avoids dataset-specific tuning.

J Additional Ablations: ViT-based SATS

J.1 Experimental Protocol

Backbones and datasets. We use the same ViT backbones and training recipes as in the main paper and report results on **CIFAR-10** and **CIFAR-100**. Unless otherwise stated, all models are trained for 350 epochs with identical data augmentation, optimisers, and learning-rate schedules.

Additional baselines. Our focus is a ranking-preserving, lightweight scalar calibrator. More expressive post-hoc alternatives (e.g., classwise or vector scaling) can correct class-conditional biases at the expense of additional degrees of freedom and potential decision changes. We include an extended-head comparison (e.g., Dirichlet-style parameterization) to illustrate this capacity–complexity trade-off and leave broader calibrator families and ensembles as future work.

Table 13: **Checkpoint size overhead of CalAttn.** We report the on-disk checkpoint size (MB) of baseline models and models augmented with CalAttn under the same serialization settings; Δ denotes the absolute increase.

| Dataset | Backbone | Variant | Size (MB) | Δ (MB) |
|---------|-----------------------|------------------|-----------|---------------|
| C-10 | ViT ₂₂₄ | baseline | 327.38 | – |
| | | + CalAttn (ours) | 327.76 | +0.38 |
| | DeiT _{small} | baseline | 82.72 | – |
| | | + CalAttn (ours) | 82.91 | +0.19 |
| | Swin _{small} | baseline | 186.16 | – |
| | | + CalAttn (ours) | 186.54 | +0.38 |
| C-100 | ViT ₂₂₄ | baseline | 327.64 | – |
| | | + CalAttn (ours) | 328.02 | +0.38 |
| | DeiT _{small} | baseline | 82.85 | – |
| | | + CalAttn (ours) | 83.04 | +0.19 |
| | Swin _{small} | baseline | 186.42 | – |
| | | + CalAttn (ours) | 186.80 | +0.38 |

Table 14: DeiT-S trained with CE+ λ Brier (without CalAttn), evaluated after TS.

| λ | ECE \downarrow | AdaECE \downarrow | ClassECE \downarrow | smECE \downarrow |
|-----------|------------------|---------------------|-----------------------|--------------------|
| 0.1 | 2.39 | 2.44 | 0.26 | 2.44 |
| 0.2 | 2.48 | 2.38 | 0.27 | 2.47 |
| 0.3 | 2.50 | 2.39 | 0.27 | 2.48 |
| 0.4 | 2.48 | 2.38 | 0.28 | 2.47 |
| 0.5–1.0 | 2.48 | 2.38 | 0.27 | 2.47 |

Calibration variants. We compare the following methods: (i) **ViT (baseline)** trained with cross-entropy; (ii) **ViT+CalAttn** (our representation-conditioned temperature head with Brier penalty); (iii) **ViT+CalAttn+TS** (post-hoc global temperature scaling on CalAttn); (iv) **ViT+CalAttn+SATS**, where SATS is applied post-hoc on top of CalAttn. SATS follows [Joy *et al.*, 2023], using a lightweight MLP that predicts a per-sample temperature from logits (and optionally the CLS embedding).

Temperature scaling. Global TS selects $T \in \{0.1, 0.2, \dots, 10.0\}$ on a held-out 5% validation split to minimise **ECE**, following [Mukhoti *et al.*, 2020a] for comparability with focal-family baselines.

SATS training. SATS is trained post-hoc on the same validation split for 10 epochs with early stopping on validation ECE. Unless stated otherwise, the input consists only of pre-softmax logits, matching [Joy *et al.*, 2023].

Metrics. We report mean \pm std over three random seeds (0,1,2) for Top-1 accuracy, negative log-likelihood (NLL), Brier score, ECE, and smECE (bandwidth $h = 0.05$).

J.2 Results

Across both datasets, CalAttn consistently reduces ECE and smECE relative to the ViT baseline without affecting Top-1 accuracy. Adding a global TS step on top of CalAttn yields the strongest improvements in all calibration metrics. SATS-only improves calibration over the baseline,

Table 15: DeiT-S trained with CE+ λ Brier+CalAttn, evaluated after TS.

| λ | ECE \downarrow | AdaECE \downarrow | ClassECE \downarrow | smECE \downarrow |
|-----------|------------------|---------------------|-----------------------|--------------------|
| 0.1 | 2.03 | 1.97 | 0.26 | 1.98 |
| 0.3–0.8 | 2.30 | 2.30 | 0.25 | 2.20 |
| 0.9 | 1.43 | 1.51 | 0.25 | 1.44 |
| 1.0 | 2.36 | 2.34 | 0.25 | 2.24 |

but underperforms CalAttn+TS, indicating that learning an representation-conditioned temperature *during* training provides a stronger inductive bias than purely post-hoc fitting. This suggests that calibrating representations during training induces a smoother uncertainty geometry than fitting a temperature regressor post-hoc, which may overfit the validation split.

Table 16: ViT (3 seeds). Mean±std on CIFAR-100 and CIFAR-10. Lower is better for losses and calibration.

| Method | CIFAR-100 | | | | | CIFAR-10 | | | | |
|--------------|------------|--------------------|--------------------|------------------|------------------|------------|--------------------|--------------------|------------------|------------------|
| | Top-1 | NLL | Brier | ECE | smECE | Top-1 | NLL | Brier | ECE | smECE |
| Baseline | 66.01±0.22 | 2.608±0.012 | 0.791±0.004 | 8.54±0.26 | 8.63±0.24 | 77.20±0.31 | 0.850±0.020 | 0.224±0.004 | 3.35±0.20 | 3.52±0.22 |
| CalAttn | 66.20±0.35 | 2.514±0.014 | 0.779±0.004 | 6.39±0.21 | 6.48±0.23 | 77.50±0.20 | 0.842±0.018 | 0.210±0.003 | 2.10±0.15 | 2.25±0.16 |
| CalAttn+TS | 67.20±0.26 | 2.489±0.011 | 0.774±0.003 | 1.42±0.12 | 1.10±0.14 | 78.10±0.25 | 0.792±0.017 | 0.202±0.003 | 0.92±0.08 | 1.01±0.09 |
| CalAttn+SATS | 66.80±0.28 | 2.519±0.015 | 0.780±0.004 | 2.70±0.15 | 3.44±0.20 | 77.70±0.34 | 0.812±0.019 | 0.206±0.003 | 1.12±0.10 | 1.20±0.11 |

Table 17: ↓ AdaECE (%) before and after applying global temperature scaling. We select T^* by minimizing validation ECE with 15 equal-width bins; parentheses report T^* . AdaECE is computed with 15 adaptive (equal-count) bins.

| Dataset | Model | Weight Decay [Guo <i>et al.</i> , 2017] | | Brier Loss [Brier, 1950] | | MMCE [Kumar <i>et al.</i> , 2018] | | Label Smooth [Szegedy <i>et al.</i> , 2016] | | Focal Loss - 53 [Mukhoti <i>et al.</i> , 2020a] | | Dual Focal [Tao <i>et al.</i> , 2023] | | CE + λ BS ($\lambda = 0.1$) | |
|--------------------------------------|--------------------------------------|--------------------------------------------|-------------------|-----------------------------|-------------------|--------------------------------------|------------------|------------------------------------------------|-------------------|----------------------------------------------------|------------------|------------------------------------------|-------------------|------------------------------------------|-------------------|
| | | Pre T | Post-T (T^*) | Pre T | Post-T (T^*) | Pre T | Post-T (T^*) | Pre T | Post-T (T^*) | Pre T | Post-T (T^*) | Pre T | Post-T (T^*) | Pre T | Post-T (T^*) |
| CIFAR-100 | ResNet-50 | 17.99 | 3.38(2.20) | 5.46 | 4.24(1.10) | 15.05 | 3.42(1.90) | 6.72 | 5.37(1.10) | 5.64 | 2.84(1.10) | 8.79 | 2.27(1.30) | 14.41 | 2.38(1.60) |
| | ResNet-110 | 19.28 | 6.27(2.30) | 6.51 | 3.75(1.20) | 18.83 | 4.86(2.30) | 9.68 | 8.11(1.30) | 10.90 | 4.13(1.30) | 11.64 | 4.48(1.30) | 19.35 | 3.51(1.80) |
| | Wide-ResNet-26-10 | 15.16 | 3.23(2.10) | 4.08 | 3.11(1.10) | 13.55 | 3.83(2.00) | 3.73 | 3.73(1.00) | 2.40 | 2.38(1.10) | 5.36 | 2.38(1.20) | 6.59 | 5.19(1.20) |
| | DenseNet-121 | 19.07 | 3.82(2.20) | 3.92 | 2.41(1.10) | 17.37 | 3.07(2.00) | 8.62 | 5.92(1.10) | 3.35 | 1.80(1.10) | 6.69 | 1.69(1.20) | 16.09 | 3.04(1.60) |
| | ViT ₂₂₄ | 13.11 | 3.34(1.30) | 2.58 | 2.56(1.10) | 11.51 | 2.33(1.30) | 3.77 | 2.32(1.10) | 5.07 | 3.41(1.10) | 3.56 | 3.56(1.00) | 6.55 | 3.54(1.50) |
| | ViT ₂₂₄ +CalAttn(Ours) | 8.25 | 1.83(1.20) | 1.93 | 2.56(1.10) | 9.04 | 2.11(1.20) | 2.12 | 2.12(1.00) | 2.60 | 2.60(1.00) | 3.73 | 2.07(1.10) | 4.01 | 1.47(1.10) |
| | DeiT _{small} | 7.46 | 3.57(1.10) | 2.26 | 2.26(1.00) | 7.88 | 2.35(1.20) | 1.67 | 1.67(1.00) | 3.18 | 3.18(1.00) | 2.01 | 2.01(1.00) | 5.93 | 2.85(1.40) |
| | DeiT _{small} +CalAttn(Ours) | 6.87 | 1.04(1.20) | 1.92 | 2.41(1.10) | 6.51 | 1.34(1.20) | 1.67 | 1.67(1.00) | 3.08 | 3.08(1.00) | 3.05 | 2.47(1.10) | 4.36 | 1.73(1.10) |
| | Swin _{small} | 3.58 | 2.52(0.90) | 2.60 | 2.60(1.00) | 3.54 | 2.75(0.90) | 9.29 | 2.56(0.80) | 10.71 | 2.71(0.80) | 8.24 | 3.16(0.80) | 4.07 | 2.93(1.20) |
| | Swin _{small} +CalAttn(Ours) | 2.20 | 2.20(1.00) | 2.95 | 2.24(1.10) | 1.97 | 1.97(1.00) | 6.55 | 2.65(0.90) | 6.10 | 3.16(0.90) | 3.85 | 3.22(0.90) | 1.75 | 1.75(1.00) |
| CIFAR-10 | ResNet-50 | 4.22 | 2.11(2.50) | 1.85 | 1.34(1.10) | 4.67 | 2.01(2.60) | 4.28 | 3.20(0.90) | 1.64 | 1.64(1.00) | 1.28 | 1.28(1.00) | 5.69 | 1.98(1.90) |
| | ResNet-110 | 4.78 | 2.42(2.60) | 2.52 | 1.72(1.20) | 5.21 | 2.66(2.80) | 4.57 | 3.62(0.90) | 1.76 | 1.32(1.10) | 1.69 | 1.42(1.10) | 6.23 | 2.88(1.90) |
| | Wide-ResNet-26-10 | 3.22 | 1.62(2.20) | 1.94 | 1.94(1.00) | 3.58 | 1.83(2.20) | 4.58 | 2.55(0.80) | 1.84 | 1.63(0.90) | 3.16 | 1.20(0.80) | 3.41 | 1.76(1.50) |
| | DenseNet-121 | 4.69 | 2.28(2.40) | 1.84 | 1.84(1.00) | 4.97 | 2.69(2.40) | 4.60 | 3.36(0.90) | 1.58 | 1.62(0.90) | 0.79 | 1.32(0.90) | 5.12 | 3.25(1.60) |
| | ViT ₂₂₄ | 7.39 | 1.37(1.30) | 2.27 | 2.27(1.00) | 3.47 | 1.23(1.10) | 1.58 | 1.58(1.00) | 8.77 | 2.24(0.70) | 4.16 | 2.27(0.90) | 3.58 | 2.68(1.40) |
| | ViT ₂₂₄ +CalAttn(Ours) | 4.74 | 1.62(1.20) | 2.68 | 1.14(1.10) | 4.35 | 1.78(1.20) | 2.74 | 1.41(0.90) | 9.96 | 2.30(0.70) | 4.52 | 3.09(0.90) | 2.17 | 1.86(1.10) |
| | DeiT _{small} | 4.41 | 1.52(1.20) | 1.97 | 1.97(1.00) | 6.01 | 1.84(1.20) | 1.66 | 1.66(1.00) | 10.62 | 3.17(0.70) | 5.11 | 3.00(0.80) | 2.97 | 1.83(1.30) |
| | DeiT _{small} +CalAttn(Ours) | 4.08 | 1.95(1.10) | 1.99 | 1.59(1.10) | 3.48 | 1.40(1.10) | 2.20 | 2.20(1.00) | 9.91 | 1.73(0.70) | 4.20 | 2.87(0.90) | 1.95 | 1.39(1.10) |
| | Swin _{small} | 1.27 | 2.00(0.90) | 1.77 | 1.77(1.00) | 1.86 | 2.42(0.90) | 6.67 | 1.41(0.80) | 15.69 | 2.28(0.60) | 8.40 | 2.57(0.70) | 1.66 | 1.40(1.20) |
| | Swin _{small} +CalAttn(Ours) | 1.66 | 1.66(1.00) | 1.17 | 1.17(1.00) | 0.97 | 0.97(1.00) | 5.94 | 1.56(0.80) | 14.98 | 1.56(0.60) | 7.40 | 2.47(0.80) | 0.88 | 0.88(1.00) |
| MNIST | ViT ₂₂₄ | 2.97 | 1.15(0.90) | 48.83 | 6.07(8.70) | 19.96 | 5.28(2.10) | 12.82 | 8.53(1.50) | 24.06 | 2.41(1.40) | 18.12 | 5.07(2.30) | 5.34 | 1.08(0.80) |
| | ViT ₂₂₄ +CalAttn(Ours) | 2.65 | 0.80(0.90) | 3.12 | 0.77(0.90) | 3.89 | 1.08(0.80) | 8.29 | 1.15(0.70) | 7.04 | 1.10(0.40) | 18.38 | 1.54(0.50) | 0.74 | 0.44(0.90) |
| | DeiT _{small} | 2.85 | 1.11(0.90) | 28.36 | 3.06(3.20) | 4.53 | 0.98(0.80) | 8.69 | 0.97(0.70) | 21.72 | 2.26(0.50) | 8.96 | 1.87(0.70) | 4.48 | 1.04(0.80) |
| | DeiT _{small} +CalAttn(Ours) | 1.17 | 1.17(1.00) | 1.08 | 1.04(0.90) | 2.22 | 1.02(0.90) | 6.20 | 1.33(0.80) | 18.28 | 1.81(0.50) | 15.90 | 2.38(0.60) | 0.91 | 0.91(1.00) |
| | Swin _{small} | 3.64 | 3.21(1.10) | 1.12 | 0.38(0.90) | 1.24 | 0.50(0.90) | 7.99 | 1.21(0.70) | 7.08 | 0.35(0.50) | 5.04 | 0.37(0.60) | 0.46 | 0.46(1.00) |
| | Swin _{small} +CalAttn(Ours) | 0.84 | 0.39(1.20) | 0.76 | 0.32(0.90) | 1.19 | 0.46(0.90) | 6.59 | 1.01(0.70) | 11.74 | 0.75(0.50) | 8.79 | 0.40(0.50) | 0.85 | 0.42(0.90) |
| Tiny-ImageNet | ViT ₂₂₄ | 4.36 | 1.73(1.10) | 4.40 | 1.67(1.10) | 4.96 | 2.39(1.20) | 2.09 | 2.28(1.10) | 3.23 | 2.23(1.10) | 2.50 | 2.68(1.10) | 1.44 | 1.39(1.10) |
| | ViT ₂₂₄ +CalAttn(Ours) | 22.11 | 3.01(1.90) | 9.18 | 0.85(1.30) | 19.84 | 3.02(1.80) | 2.05 | 1.98(1.10) | 1.68 | 1.23(1.10) | 13.57 | 1.10(1.40) | 1.01 | 0.78(1.10) |
| | DeiT _{small} | 13.04 | 2.25(1.40) | 2.38 | 2.04(1.10) | 13.66 | 1.37(1.50) | 1.71 | 1.71(1.00) | 10.26 | 2.39(1.70) | 9.37 | 1.86(1.50) | 1.43 | 1.29(1.10) |
| | DeiT _{small} +CalAttn(Ours) | 2.12 | 1.77(1.40) | 2.26 | 1.47(1.20) | 2.61 | 1.07(1.50) | 2.29 | 1.35(1.10) | 2.39 | 1.26(1.30) | 1.86 | 1.41(1.30) | 0.95 | 0.83(1.20) |
| | Swin _{small} | 3.48 | 2.54(0.90) | 1.05 | 0.54(0.90) | 2.15 | 2.15(1.00) | 4.98 | 2.44(0.90) | 4.66 | 2.69(0.90) | 4.96 | 2.62(0.90) | 0.91 | 0.91(1.00) |
| Swin _{small} +CalAttn(Ours) | 2.84 | 1.63(1.10) | 0.84 | 1.12(1.10) | 1.57 | 1.57(1.00) | 2.62 | 2.62(1.00) | 2.37 | 2.37(1.00) | 2.29 | 2.29(1.00) | 0.82 | 0.24(0.90) | |

Table 18: ↓ Classwise-ECE (%) before and after applying global temperature scaling (15 bins).

| Dataset | Model | Weight Decay [Guo <i>et al.</i> , 2017] | | Brier Loss [Brier, 1950] | | MMCE [Kumar <i>et al.</i> , 2018] | | Label Smooth [Szegedy <i>et al.</i> , 2016] | | Focal Loss - 53 [Mukhoti <i>et al.</i> , 2020a] | | Dual Focal [Tao <i>et al.</i> , 2023] | | CE + λ BS ($\lambda = 0.1$) | |
|-----------|--------------------------------------|--------------------------------------------|-------------------|-----------------------------|------------------|--------------------------------------|-------------------|------------------------------------------------|-------------------|----------------------------------------------------|-------------------|------------------------------------------|-------------------|------------------------------------------|-------------------|
| | | Pre T | Post-T (T^*) | Pre T | Post-T (T^*) | Pre T | Post-T (T^*) | Pre T | Post-T (T^*) | Pre T | Post-T (T^*) | Pre T | Post-T (T^*) | Pre T | Post-T (T^*) |
| CIFAR-100 | ResNet-50 | 0.39 | 0.22(2.20) | 0.21 | 0.22(1.10) | 0.34 | 0.22(1.90) | 0.21 | 0.22(1.10) | 0.21 | 0.20(1.10) | 0.24 | 0.22(1.30) | 0.34 | 0.23(1.60) |
| | ResNet-110 | 0.42 | 0.21(2.30) | 0.22 | 0.23(1.20) | 0.41 | 0.22(2.30) | 0.25 | 0.23(1.30) | 0.27 | 0.22(1.30) | 0.28 | 0.21(1.30) | 0.43 | 0.23(1.80) |
| | Wide-ResNet-26-10 | 0.34 | 0.21(2.10) | 0.19 | 0.20(1.10) | 0.31 | 0.21(2.00) | 0.20 | 0.20(1.00) | 0.18 | 0.20(1.10) | 0.19 | 0.20(1.20) | 0.33 | 0.30(1.20) |
| | DenseNet-121 | 0.42 | 0.22(2.20) | 0.21 | 0.21(1.10) | 0.39 | 0.23(2.00) | 0.23 | 0.21(1.10) | 0.20 | 0.21(1.10) | 0.22 | 0.21(1.20) | 0.37 | 0.25(1.60) |
| | ViT ₂₂₄ | 0.43 | 0.26(1.30) | 0.29 | 0.28(1.10) | 0.40 | 0.26(1.30) | 0.27 | 0.25(1.10) | 0.33 | 0.29(1.10) | 0.28 | 0.28(1.00) | 0.30 | 0.27(1.50) |
| | ViT ₂₂₄ +CalAttn(Ours) | 0.34 | 0.27(1.20) | 0.35 | 0.34(1.10) | 0.36 | 0.29(1.20) | 0.28 | 0.28(1.00) | 0.30 | 0.30(1.00) | 0.29 | 0.26(1.10) | 0.29 | 0.26(1.10) |
| | DeiT _{small} | 0.33 | 0.28(1.10) | 0.28 | 0.28(1.00) | 0.33 | 0.26(1.20) | 0.26 | 0.26(1.00) | 0.29 | 0.29(1.00) | 0.27 | 0.27(1.00) | 0.33 | 0.30(1.40) |
| | DeiT _{small} +CalAttn(Ours) | 0.33 | 0.27(1.20) | 0.36 | 0.36(1.10) | 0.32 | 0.26(1.20) | 0.28 | 0.28(1.00) | 0.29 | 0.29(1.00) | 0.28 | 0.26(1.10) | 0.32 | 0.29(1.10) |
| | Swin _{small} | 0.28 | 0.28(1.00) | 0.35 | 0.35(1.00) | 0.27 | 0.27(0.90) | 0.33 | 0.30(0.80) | 0.33 | 0.29(0.80) | 0.33 | 0.31(0.80) | 0.30 | 0.29(1.20) |
| | Swin _{small} +CalAttn(Ours) | 0.28 | 0.28(1.00) | 0.41 | 0.40(1.10) | 0.27 | 0.27(1.00) | 0.30 | 0.28(0.90) | 0.28 | 0.27(0.90) | 0.27 | 0.28(0.90) | 0.27 | 0.27(1.00) |
| CIFAR-10 | ResNet-50 | 0.87 | 0.37(2.50) | 0.46 | 0.39(1.10) | 0.97 | 0.55(2.60) | 0.80 | 0.54(0.90) | 0.41 | 0.41(1.00) | 0.45 | 0.45(1.00) | 1.18 | 0.58(1.90) |
| | ResNet-110 | 1.00 | 0.54(2.60) | 0.55 | 0.46(1.20) | 1.08 | 0.60(2.80) | 0.75 | 0.50(0.90) | 0.48 | 0.46(1.10) | 0.46 | 0.52(1.10) | 1.31 | 0.68(1.90) |
| | Wide-ResNet-26-10 | 0.68 | 0.34(2.20) | 0.37 | 0.37(1.00) | 0.77 | 0.41(2.20) | 0.95 | 0.37(0.80) | 0.44 | 0.34(0.90) | 0.82 | 0.33(0.80) | 1.24 | 1.12(1.50) |
| | DenseNet-121 | 0.98 | 0.54(2.40) | 0.43 | 0.43(1.00) | 1.02 | 0.53(2.40) | 0.75 | 0.48(0.90) | 0.43 | 0.41(0.90) | 0.40 | 0.41(0.90) | 1.17 | 0.58(1.60) |
| | ViT ₂₂₄ | 1.68 | 0.78(1.30) | 1.15 | 1.15(1.00) | 0.97 | 0.70(1.10) | 0.73 | 0.73(1.00) | 1.76 | 1.32(0.70) | 0.96 | 0.89(0.90) | 1.44 | 1.32(1.40) |
| | ViT ₂₂₄ +CalAttn(Ours) | 1.33 | 0.85(1.20) | 1.45 | 1.29(1.10) | 1.42 | 0.99(1.20) | 1.25 | 1.05(0.90) | 2.09 | 1.33(0.70) | 1.34 | 1.29(0.90) | 1.13 | 1.10(1.10) |
| | DeiT _{small} | 1.24 | 0.74(1.20) | 1.41 | 1.41(1.00) | 1.35 | 0.71(1.20) | 0.88 | 0.88(1.00) | 2.12 | 1.05(0.70) | 1.19 | 1.08(0.80) | 1.26 | 0.97(1.30) |
| | DeiT _{small} +CalAttn(Ours) | 1.16 | 0.89(1.10) | 0.93 | 0.86(1.10) | 1.13 | 0.91(1.10) | 0.97 | 0.97(1.00) | 1.98 | 1.14(0.70) | 1.21 | 1.16(0.90) | 0.93 | 0.86(1.10) |
| | Swin | | | | | | | | | | | | | | |